Journal of Medicinal Chemistry

Article

Discovery of Potent Human Glutaminyl Cyclase Inhibitors as Anti-Alzheimer's Agents based on Rational Design

Van-Hai Hoang, Phuong-Thao Tran, Minghua Cui, Van T.H. Ngo, Jihyae Ann, Jongmi Park, Jiyoun Lee, Kwanghyun Choi, Hanyang Cho, Hee Kim, Heejin Ha, Hyun-Seok Hong, Sun Choi, Young-Ho Kim, and Jeewoo Lee

J. Med. Chem., **Just Accepted Manuscript** • DOI: 10.1021/acs.jmedchem.7b00098 • Publication Date (Web): 24 Feb 2017

ACS Publications

Journal of Medicinal Chemistry is published by the American Chemical Society. 1155 Sixteenth Street N.W., Washington, DC 20036

Discovery of Potent Human Glutaminyl Cyclase Inhibitors as Anti-Alzheimer's Agents based on Rational Design

Van-Hai Hoang,[†] Phuong-Thao Tran,[†,⊥] Minghua Cui,[‡] Van T.H. Ngo,[†] Jihyae Ann,[†] Jongmi Park,[‡] Jiyoun Lee,[∥] Kwanghyun Choi,[§] Hanyang Cho,[§] Hee Kim,[§] Hee-Jin Ha,[§] Hyun-Seok Hong,[§] Sun Choi,[‡] Young-Ho Kim,[§] Jeewoo Lee*[,†]

[†] Laboratory of Medicinal Chemistry, Research Institute of Pharmaceutical Sciences, College of Pharmacy, Seoul National University, Seoul 08826, Republic of Korea

[‡] National Leading Research Laboratory of Molecular Modeling & Drug Design, College of Pharmacy and Graduate School of Pharmaceutical Sciences, Ewha Womans University, Seoul 03760, Republic of Korea

[§] Medifron DBT, Sandanro 349, Danwon-Gu, Ansan-City, Gyeonggi-Do 15426, Republic of Korea

[∥] Department of Global Medical Science, Sungshin University, Seoul 01133, Republic of Korea

[⊥] Department of Pharmaceutical Chemistry, Hanoi University of Pharmacy, Hanoi, Vietnam

ABSTRACT

Glutaminyl cyclase (QC) has been implicated in the formation of toxic amyloid plaques by generating the *N*-terminal pyroglutamate of β-amyloid peptides (pGlu-Aβ), thus may participate in the pathogenesis of Alzheimer's disease. We designed a library of glutamyl cyclase (QC) inhibitors based on the proposed binding mode of the preferred substrate, $A\beta_{3E\text{-}42}$. An *in vitro* structure-activity relationship study identified several excellent QC inhibitors demonstrating 5- to 40-fold increases in potency compared to a known QC inhibitor. When tested in mouse models of Alzheimer's disease (AD), compound **212** significantly reduced the brain concentrations of pyroform Aβ and total Aβ and restored cognitive functions. This potent Aβ-lowering effect was achieved by incorporating an additional binding region into our previously established pharmacophoric model, resulting in strong interactions with the carboxylate group of Glu327 in the QC binding site. Our study offers useful insights in designing novel QC inhibitors as a potential treatment option for AD.

■ INTRODUCTION

Alzheimer's disease (AD) and related dementias are the leading cause of disabilities in old age and have become enormous socioeconomic burdens to many countries with rapidly growing elderly populations. The currently available treatment options for AD, such as acetylcholinesterase inhibitors (AChEI) and *N*-methyl-D-aspartate (NMDA) receptor antagonists, offer only limited symptomatic relief, rather than modifying the disease course. Among the various alternatives that have been extensively investigated, β-amyloid (Aβ)-targeted therapies have been the center of attention because many research findings indicated that elevated levels of Aβ peptides in the brain promote the formation of amyloid plaques and neuronal death.[1] What causes the elevated levels of Aβ peptides is still under debate, but either facilitating the clearance or suppressing the formation of Aβ is likely to reduce amyloid burdens in the brain, possibly slowing down the neurodegenerative process. Unfortunately, several Aβ-lowering drugs based on this premise, such as bapineuzumab, solanezumab, and semagacestat, have failed to provide significant therapeutic benefits in clinical trials. One possible explanation for this recent failure is that the brain Aβ peptides are a heterogeneous mixture of peptides, each form of which displays different structural and functional features.[2,3] Given that Aβ peptides participate in such diverse physiological processes including neurogenesis,[4] neuronal survival,[5-7] oxidative stress,[8,9] and innate immunity,[10] targeting specific forms of Aβ peptides that are prone to aggregation and are neurotoxic may provide a more effective therapy.

Aβ peptides are generated by the proteolytic cleavage of the amyloid precursor protein (APP), a transmembrane glycoprotein. Depending on the sequential cleavage sites, Aβ peptides with 30-51 amino acid residues are produced. $A\beta_{1-40}$ and $A\beta_{1-42}$ are the most abundant isoforms in the human brain and are thought to be the major initiators of AD pathogenesis. The brains of

AD patients also contain a significant amount of *N*-terminally truncated species, such as $A\beta_{n\text{-}40/42}$, where n ranges from 2 to 11.[11-13] Many studies have found that these *N*-terminally truncated species are further cyclized to form pyroglutamate (pGlu)-Aβ. Due to their increased hydrophobicity, pGlu-Aβ peptides are prone to rapid aggregation and are much more resistant to proteolytic degradation. In fact, $A\beta_{3(pE)\text{-}42}$ constitutes approximately 15-20% of the total $A\beta_{42}$ and is deposited in the center of senile plaques in the brains of AD patients.[14-16] It has been reported that pGlu-Aβ peptides are more neurotoxic than $A\beta_{1\text{-}40}$ and $A\beta_{1\text{-}42}$ and act as a seed for amyloid and tau plaques.[17-19]

The pGlu-Aβ peptides are generated by glutaminyl cyclase (QC). Mammalian QC is mainly found in the pituitary, hypothalamus, and brain and participates in the maturation of neuropeptides and hormones.[20-22] Notably, QC is overexpressed in the brains of AD patients and animal models,[23,24] and the knock-out of QC rescued the cognitive function in AD model mice.[25] Small molecule QC inhibitors also reduced brain pGlu-Aβ levels and Aβ plaques,[26] in addition to decreasing gliosis and restoring memory deficits in AD mice.[24] In addition, the results from a recent phase I trial indicate that QC inhibitors are well tolerated and metabolically safe for both young and elderly patients,[27] suggesting that the inhibition of QC offers an alternative approach to conventional Aβ-lowering agents.

In contrast to the emerging importance of QC in AD pathogenesis, relatively few QC inhibitors have been reported so far.[28-32] In general, these inhibitors share two distinct structural features: first, a zinc-binding moiety, such as imidazole, that can bind to the active site zinc ion and second, a large hydrophobic residue that can occupy the penultimate position to the *N*-terminal glutamine. Previously, our group designed a series of QC inhibitors based on this

general scaffold, which we divided into three pharmacophoric regions: A-region representing the zinc-binding group, B-region containing a hydrogen bond donor, and C-region mimicking the aromatic ring of the phenylalanine side chain.[32] We studied the structure-activity relationship specifically focused on the C-region, while having 5-methylimidazole in the A-region and a propylthiourea moiety in the B-region, based on the structure of the previously reported QC inhibitor, compound **1** (**Figure 1**).[28] Although we found a promising candidate with an IC_{50} value of 58 nM in our previous study, we wanted to further expand our library of QC inhibitors and to study their SAR as well as their *in vivo* activity. To identify an additional pharmacophore, we turned our attention to the antepenultimate Arg of $A\beta_{3E\text{-}42}$. While the substrate specificity of this specific position has not been clearly elucidated, we speculated that the additional side chain might be able to act as a positional anchor to provide enhanced binding interactions. Therefore, we designed a novel scaffold that has an additional pharmacophoric region D, as described in **Figure 1**. These new series of compounds contain various amine-type functional groups in the D-region, which mimic the guanidine moiety of Arg. In this work, we synthesized newly designed QC inhibitors focused on the D-region and investigated their SAR based on *in vitro* inhibition for human QC. Furthermore, we evaluated the efficacy of the selected inhibitors by measuring their ability to reduce the formation of $A\beta_{3(pE)\text{-}42}$ and to prevent memory impairment in AD model mice. Finally, we analyzed the specific binding interactions between the selected inhibitors and the QC active site by performing molecular docking studies.

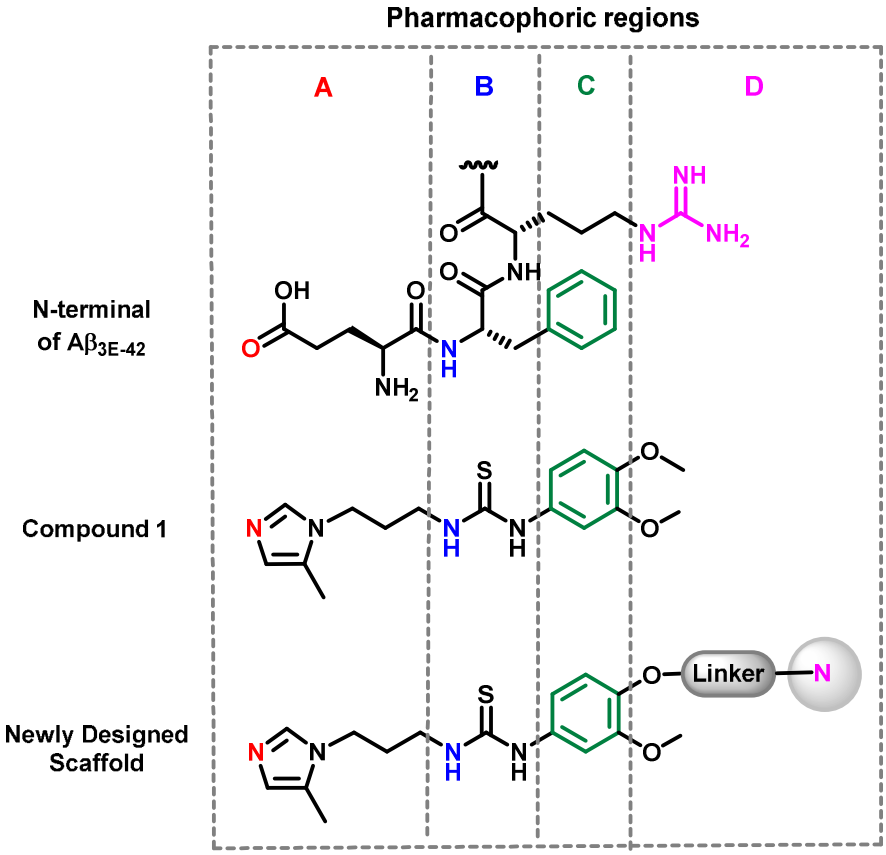

Figure 1. Newly designed scaffold for QC inhibitors

■ RESULTS AND DISCUSSION

Chemistry.

To synthesize compounds with the newly designed scaffold that includes the D-region, we first synthesized a library of 1-alkyloxy-2-methoxy-4-nitrobenzene fragments, as shown in **Schemes 1-3**. The syntheses of 1-acyclic and cyclic aminoalkyloxy-2-methoxy-4-nitrobenzene derivatives are described in **Scheme 1**. The Williamson reaction of 4-nitroguaialcol **2** with dibromoalkanes followed by *N*-alkylation provided piperidine, morpholine and piperazine derivatives **6-17**. 4-Substituted piperidinyl derivatives, **18-20**, were synthesized by the Mitsunobu reaction of **2** with corresponding 4-(hydroxyalkyl)piperidine fragments,[33, 34] followed by an *N*-

Boc deprotection reaction to afford **21** and **23**. Compounds **21** and **23** were then reductively methylated to provide **22** and **24**. Acyclic aminoalkyl derivatives**, 25-28**, were synthesized by Williamson or Mitsunobu reactions with **2**. Alkyl phthalimide intermediates, **29** and **30**, were prepared from **2** and deprotected to give primary amines **31** and **32**, which were converted to compound **33** by reductive amination and to compounds **38-41** by monoalkylation using 2-nitrobenzenesulfonamide[35] as a protecting group, respectively. 1-Heteroarylalkyloxy-2-methoxy-4-nitrobenzene fragments were prepared as described in **Scheme 2**. The Sonogashira reaction of aryl bromides **42-45, 47**[36] with corresponding terminal alkynes provided the alkyne intermediates **50-58**, which were further reduced and underwent a Mitsunobu reaction to afford **70-74**, **76-79**. Compound **75** was prepared from commercially available **48** by reduction and protection followed by the Williamson reaction. 1-Pyridinylalkoxy-2-methoxy-4-nitrobenzene fragments were synthesized as described in **Scheme 3**. The C-alkylation of picolines and aminopicolines with bromoalkane derivatives or diethylcarbonate provided chloroethyl, TBS-protected hydroxyalkyl, and ethoxycarbonyl intermediates (**85-89, 92-93**). Chloroalkyl intermediates (**85-87**) were conjugated with 4-nitroguaiacol via the Williamson reaction to produce compounds **96-98**, while TBS-protected hydroxyalkyl intermediates (**88-89**) were first deprotected with TBAF, and subsequently conjugated with 4-nitroguaiacol via the Mitsunobu reaction to yield compounds **99-100**. The ethoxycarbonyl group in compounds **92-93** was first reduced to an ethylalcohol group (**94-95**) by using LAH, and further conjugated with 4-nitroguaiacol via the Mitsunobu reaction to generate compounds **101-102**.

As described in **Scheme 4**, all of the synthesized 1-alkyloxy-2-methoxy-4-nitrobenzene fragments were reduced to corresponding amines, **103-145**, which were subsequently converted to isothiocyanate and coupled with 3-(5-methyl-1*H*-imidazol-1-yl)propan-1-amine to afford the final thiourea compounds *in situ*. Compounds **146-166** were further subjected to *N*-Boc

deprotection, while compounds **167** and **168** were reacted with hydrazine to deprotect a phthalimide group, yielding primary amine final compounds (**172-174, 191-193, 197-198, 203-205, 210-211, 214-216, 219-220**) as well as amine intermediates (**169-171, 199, 212**). The final modification of the primary amine group of these intermediates generated acetylated (**178, 213**), guanidinylated (**179**), and methylated (**202**) analogues. The 2-chloropyrimidine derivatives (**180-184**) were synthesized via the nucleophilic substitution of the amine intermediates to afford the corresponding final compounds.

Scheme 1. Synthesis of alkyl D-region[a]

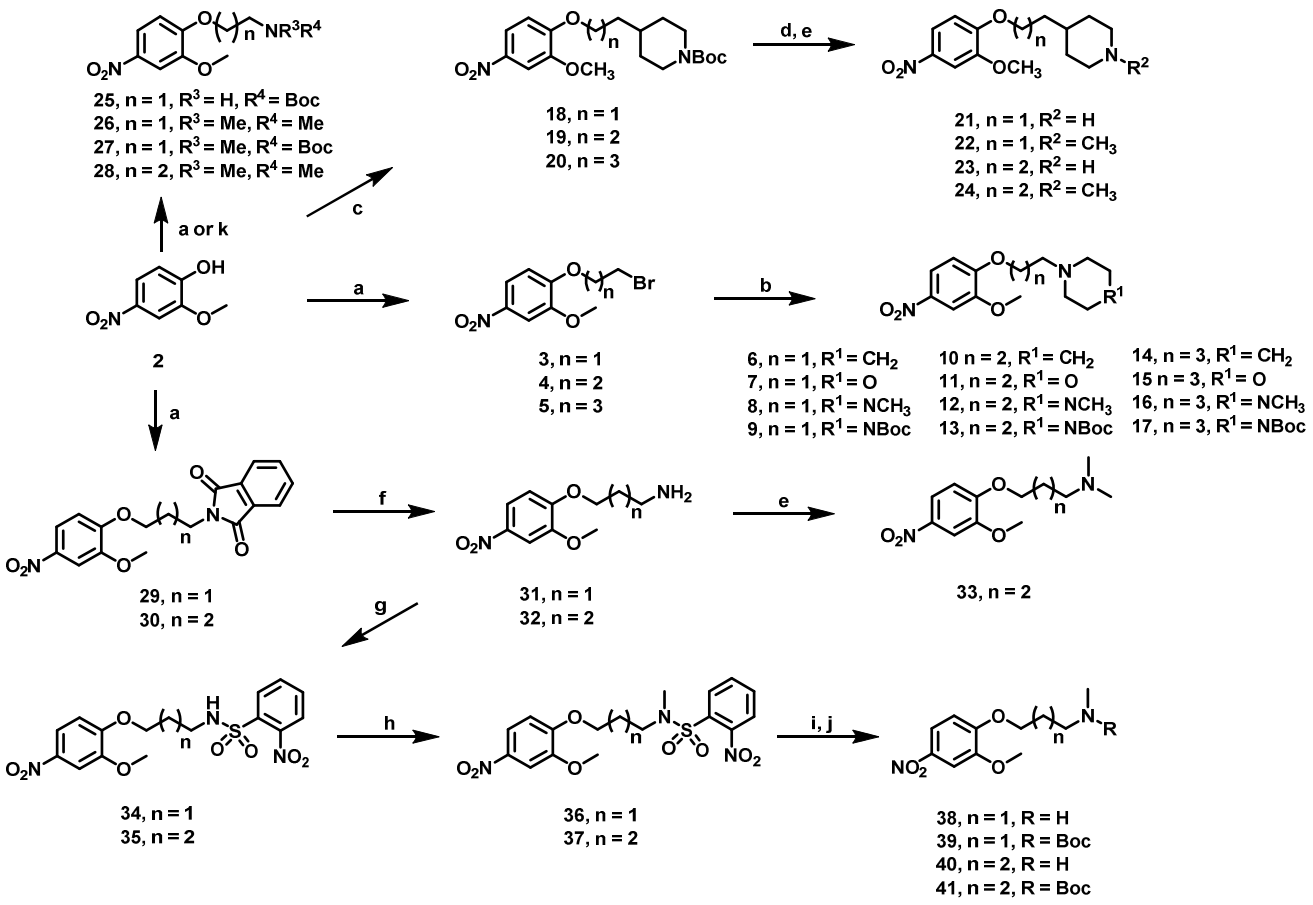

[a] Reagents and conditions: (a) Bromoalkyl derivatives, K_2CO_3, DMF, 100°C, 1 h for **25**, **26**, and **28**; (b) DMF, base (piperidine, morpholine, 1-methylpiperazine or *N*-Boc piperazine), heat; (c) 4-(hydroxyalkyl)piperidine, DEAD, PPh_3, DCM, r.t, 2 h; (d) TFA, DCM, r.t, overnight; (e) $(HCHO)_n$, $ZnCl_2$,

DCM, r.t, 1 h; then $NaBH_4$, reflux, overnight; (f) $N_2H_4.H_2O$, EtOH, r.t, overnight; (g) 2-nitrobenzenesulfonyl chloride, TEA, DCM, r.t, 5 h; (h) CH_3I, NaH, THF, r.t, overnight; (i) thiophenol, K_2CO_3, MeCN, r.t, overnight; (j) Boc_2O, Et_3N, DCM, r.t, 2 h; (k) $HO(CH)_2N(CH_3)Boc$, DEAD, PPh_3, DCM, r.t, 2 h for **27**.

Scheme 2. Synthesis of aryl D-region[a]

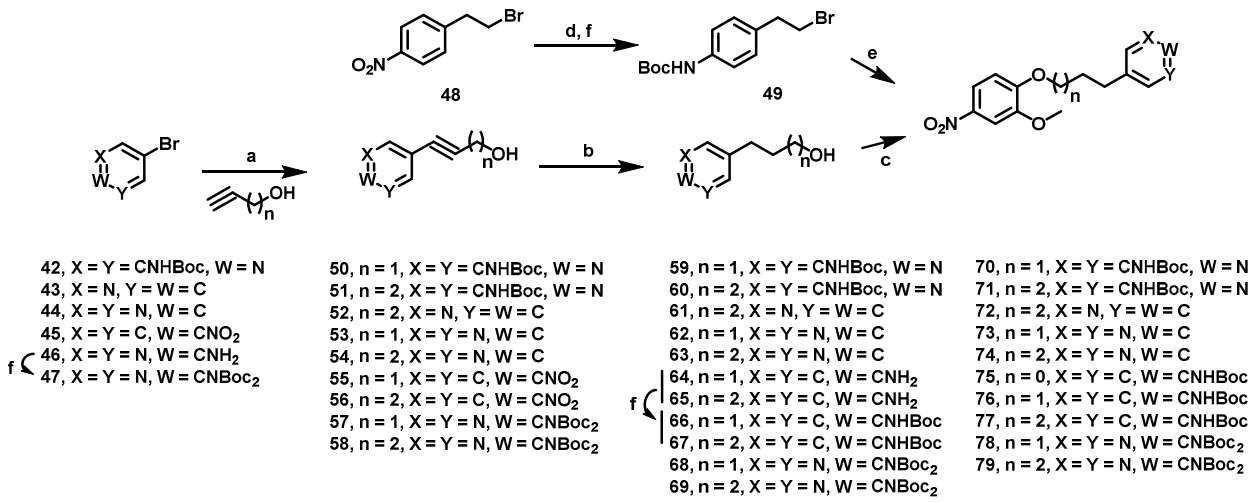

[a] Reagents and conditions: (a) CuI, $Pd(PPh_3)_4$, Et_3N, DCM, 50°C, overnight or alkyn-1-ol, DMF, Et_3N, $(Ph_3P)_2PdCl_2$, CuI, r.t, 15 h; (b) Pd/C, MeOH, H_2, r.t, overnight; (c) 4-nitroguaiacol, DEAD, PPh_3, DCM, r.t, 2 h; (d) $HCOONH_4$, Zn, MeOH, r.t, 15 min; (e) 4-nitroguaiacol, Cs_2CO_3, DMF, 100°C; (f) Boc_2O, Et_3N, DCM, r.t, overnight.

Scheme 3. Synthesis of aryl D-region[a]

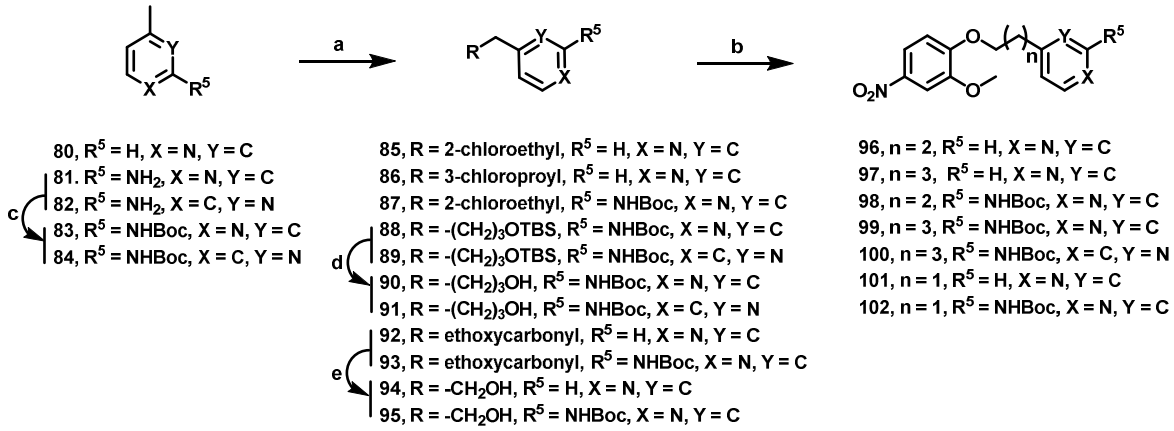

[a] Reagents and conditions: (a) bromoalkane derivatives or diethylcarbonate, *n*-BuLi, THF, -78 °C; (b) 4-nitroguaiacol, K_2CO_3, DMF, 100°C, 1 h or 4-nitroguaiacol, DEAD, Ph_3P, DCM, r.t; (c) Boc_2O, *t*-BuOH, r.t, overnight; (d) TBAF, THF, r.t, 2 h; (e) LAH, THF, 0°C, 1 h.

Scheme 4. Synthesis of final QC inhibitors[a]

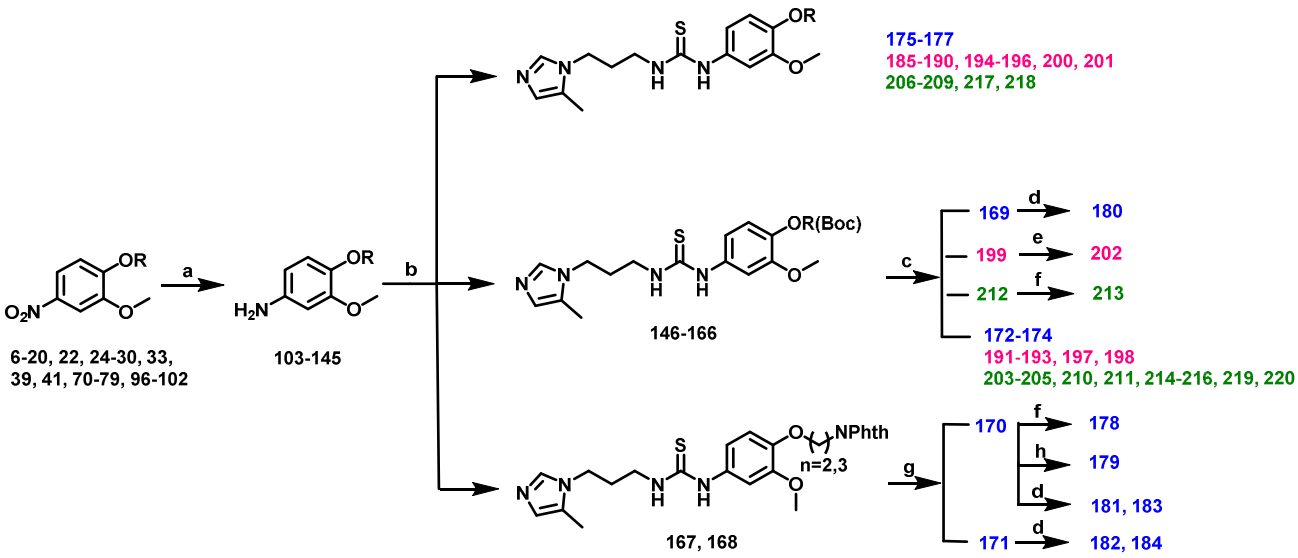

[a] Reagents and conditions: (a) Pd/C, H_2, MeOH, r.t, overnight; (b) 3-(5-methyl-1*H*-imidazol-1-yl)propan-1-amine, TCDI, Et_3N, DCM, r.t-40°C, overnight; (c) TFA, DCM, r.t, 2 h; (d) 2-chloropyrimidine derivatives, EtOH, Et_3N, reflux, 2 days; (e) $(HCHO)_n$, $ZnCl_2$, DCM, r.t, 1 h; then $NaBH_4$, reflux, overnight; (f) Ac_2O, pyridine, MC, r.t, 4-5 h; (g) $N_2H_4.H_2O$, EtOH, r.t, overnight; (h) 1*H*-pyrazole-1-carboxamidine-HCl, *i*Pr_2EtN, MeOH, r.t-50°C, 2 h.

In vitro QC Inhibition.

To evaluate the biological activity of the compound library, we determined the QC inhibition of each compound by using a fluorogenic substrate, Gln-AMC (L-glutamine 7-amido-4-methylcoumarin), and pyroglutamyl peptidase (pGAP) as an auxiliary enzyme.[37] In this assay, QC first converts Gln-AMC into pGlu-AMC, which is then hydrolyzed by pGAP to generate AMC. AMC can be detected by measuring the fluorescence at the excitation and emission wavelengths of 380 and 460 nm. These results are summarized in **Table 1-3**, along with the IC_{50} value of compound **1** (IC_{50} = 29.2 nM) for comparison.

First, we analyzed the structure-activity relationship of aliphatic amines in the D-region, as shown in **Table 1**. The group I (**169-184**) contain various terminal amine, amide, guanidine, and pyrimidylamine functional groups, while having an aliphatic linker that was varied in length. In general, compounds with a 2-carbon linker (**169**, **172**, **175**, **180**) showed a similar activity to **1**, whereas compounds with a 3-carbon (**170**, **173**, **176, 181, 183**) or 4-carbon (**171**, **174**, **177, 182, 184**) linker demonstrated more potent inhibition. In particular, **170**, **177** and **182** were found to be 6-8-fold more potent than **1**, having IC_{50} values of 5.3, 3.7, and 5.7 nM, respectively. Among the various terminal functional groups, amines and pyrimidylamines showed greater inhibition than amide or guanidine groups, suggesting that the electron density in this region might control the binding interactions rather than the size or number of hydrogens. Furthermore, compound **182** showed 3-fold more potent inhibition than compound **184**, which contained an extra fluorine atom in the pyrimidylamine ring, supporting our hypothesis.

Table 1. IC_{50} values for inhibition of *h*QC by benzocyclic compounds (Group I)

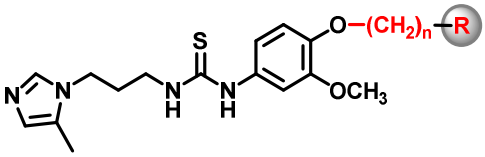

Compound	R	n	IC_{50} (nM)[a]
1			29.2 (±4.0)
169		2	30.2 (±4.3)
170	*–NH_2	3	5.3 (±1.0)
171		4	13.8 (±3.1)
172		2	38.7 (±7.1)
173	*–N(H)	3	6.9 (±1.4)
174		4	16.2 (±2.1)
175	*–N	2	38.6 (±4.3)

176		3	13.0	(±1.7)
177		4	3.7	(±1.1)
178		3	40.8	(±2.4)
179	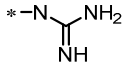	3	41.2	(±8.2)
180		2	39.4	(±10.4)
181	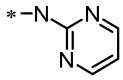	3	17.5	(±2.3)
182		4	5.7	(±2.8)
183	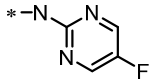	3	18.5	(±3.8)
184		4	17.5	(±4.1)

[a] The values indicate the mean of at least three experiments.

Next, we investigated the SAR of the cyclic amine-containing compounds, group II, as shown in **Table 2**. Interestingly, all the compounds in this group proved to be highly potent inhibitors, with IC_{50} values ranging from 0.7 to 24.7 nM, regardless of the type of cyclic amine and the length of the linker. In particular, 1-piperazinyl analogs (**191-193**) appeared to be the most potent in this group, with compound **191** demonstrating an IC_{50} value of 0.7 nM, is was 42-fold more potent than **1**. Both nitrogen atoms in the piperazine appeared to be important in binding interaction, because removing any one of either nitrogen reduced inhibitory activity as observed in the 1-piperidinyl (**185-187**), 4-morpholinyl (**188-190**), 4-piperidinyl (**197, 199**) except **198** (n=3), and 4-(1-methylpiperadinyl) (**200-202**) analogues. In addition, the 4-NH hydrogen might play a crucial role for favorable binding interactions, because the 1-piperidinyl (**185-187**) analogues were much less potent than the 4-piperidinyl analogues (**197-199**) as well as the 1-piperazinyl analogues (**191-193**). This apparent importance of the NH at the 4-position is not observed with n =3 derivatives (**186, 189, 192, 195, 198**, and **201**), suggesting that the

distance between the R-group and C-region also affects the hydrogen bond interaction of the 4-NH.

Table 2. IC_{50} values for inhibition of *h*QC by benzocyclic compounds (Group II)

Compound	R	n	IC_{50} (nM)[a]
185	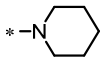	2	24.7 (±3.5)
186		3	13.4 (±1.1)
187		4	12.5 (±1.7)
188	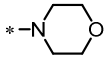	2	12.5 (±2.9)
189		3	14.1 (±0.9)
190		4	9.2 (±2.1)
191	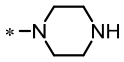	2	0.7 (±0.4)
192		3	11.4 (±2.3)
193		4	4.8 (±1.0)
194	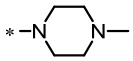	2	7.3 (±1.9)
195		3	11.7 (±1.0)
196		4	8.2 (±0.4)
197	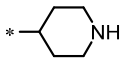	2	13.8 (±0.7)
198		3	7.2 (±1.4)
199		4	7.8 (±1.8)
200	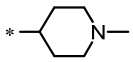	2	4.6 (±1.4)
201		3	20.2 (±3.8)
202		4	12.3 (±2.5)

[a] The values indicate the mean of at least three experiments.

We examined the QC inhibition of compounds with aryl amines and nitrogen-containing heterocycles, group III, as demonstrated in **Table 3**. All three aniline analogs (**203**-**205**) appeared to be potent inhibitors, regardless of the length of the linker, with IC_{50} values ranging from 7.7 to

9.0 nM. Within this group, the length of the alkyl linker does not significantly affect the inhibitory effects; rather, the position of nitrogen in the heterocycle seems to be crucial for favorable binding interactions, as was also observed for the compounds in group B. For example, 3-pyridyl analogue (**209**, IC_{50} = 19.8 nM) was less potent than the 4-pyridyl surrogate (**208**, IC_{50} = 9.1 nM). Among the group C compounds, **212**, a 4-(2-aminopyridyl) analogue with a 4-carbon linker, was the most potent inhibitor, having an IC_{50} value of 4.5 nM. In contrast, compound **216**, a positional isomer of **212**, exhibited much less potent inhibition (IC_{50} = 19.3 nM), again supporting that the binding direction or position of nitrogen atoms in the heterocycle is particularly important. In addition, to confirm the selectivity of compound **212**, we also determined the IC_{50} value for isoQC, an isozyme of QC with a differential substrate specificity.[38, 39] The IC_{50} value of **212** for isoQC was 502 nM, which was more than 100-fold greater than the IC_{50} value for QC, indicating that compound **212** is highly specific for QC. 5-Pyrimidinyl (**217**, **218**) and 5-(2-aminopyrimidinyl) (**219**, **220**) analogues were found to be slightly less potent than pyridine analogs.

Table 3. IC_{50} values for inhibition of *h*QC by benzocyclic compounds (Group III)

Compound	R	n	IC_{50} (nM)[a]
203	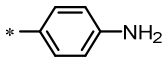	2	7.7 (±1.4)
204		3	9.0 (±1.1)
205		4	8.3 (±0.8)
206	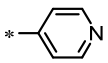	2	23.5 (±5.2)
207		3	14.4 (±4.4)
208		4	9.1 (±2.8)
209	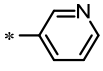	4	19.8 (±4.5)
210	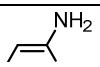	2	5.5 (±1.9)

211		3	10.7 (±2.5)
212		4	4.5 (±1.4)
213	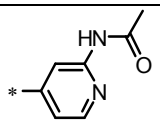	4	19.0 (±4.6)
214	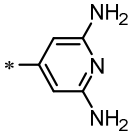	3	16.6 (±1.2)
215		4	15.3 (±3.1)
216	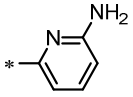	4	19.3 (±4.7)
217	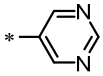	3	35.5 (±6.6)
218		4	21.3 (±4.0)
219	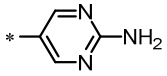	3	20.5 (±1.9)
220		4	18.4 (±1.4)

[a] The values indicate the mean of at least three experiments.

In vivo activity.

Based on the *in vitro* activity, we selected the eight most potent compounds, which demonstrated IC_{50} values less than ca. 5 nM, along with compound **1** as a control for further animal studies. We first examined the cytotoxicity of each compound in an immortalized hippocampal neuronal cell line (HT-22) and found that all compounds were non-toxic at a 10 μM concentration. For the acute model studies, we injected human $A\beta_{3\text{-}40}$ (5 μg) and each compound (25 mg/kg) into deep cortical/hippocampus of ICR mice (male, six weeks old). On the next day, the inhibitory activities were determined by measuring the levels of human $A\beta_{N3pE\text{-}40}$ in the brain extracts of the mice. As described in **Table 4**, compounds **170**, **191**, and **212** suppressed more than 60% of the formation of $A\beta_{N3pE\text{-}40}$ compared to the vehicle control, while compound **1** showed 41.6% inhibition. Specifically, compound **191**, which showed the most potent activity *in vitro*, also demonstrated the most potent $A\beta_{N3pE\text{-}40}$ lowering effects (**Table 4, Figure 2a**).

Table 4. QC inhibition in acute model studies *in vivo*.[a]

	In vitro IC_{50} (nM)	Cytotoxicity at 10 μM (% of control)	% inhibition of human $A\beta_{N3pE-40}$ formation (deep cortical/hippocampus injected)	% inhibition of human $A\beta_{N3pE-40}$ formation (i.p. injected)	PAMPA (-logPe)
1	29.2 (21.5)[b]	~100	41.6	NE	6.3
170	5.3	~100	64.6	NE	6.2
177	3.7	~100	35.7		
182	5.7	~100	27.3		
191	0.7	~100	77.2	3.6	6.1
193	4.8	~100	29.2		
200	4.6	~100	18.7		
210	5.5	~100	38.0		
212	4.5 (12.6)[b]	~100	66.1	54.7	4.5

[a] 5 μL of human $A\beta_{3-40}$ in PBS (1 μg/μL) was injected into the deep cortical/hippocampus to 5 weeks old ICR mice (25 g, n = 4, male) using a stereotaxic frame to induce acute Aβ toxicity. Test compounds were administrated via icv or ip injection. Sandwich ELISA was performed for the quantification of the brain $A\beta_{N3pE-40}$; [b] IC_{50} values were measured additionally by using mouse QC.

Next, we performed another acute model study by intraperitoneally (i.p.) injecting the three most potent compounds (**170**, **191**, and **212**) to assess their *in vivo* efficacy, which can be translated to the ability to penetrate the blood-brain barrier (BBB). Again, human $A\beta_{3-40}$ was injected deep cortical/hippocampus prior to the i.p. administration of each inhibitor into ICR mice. The inhibitory activities were estimated by measuring the levels of human $A\beta_{N3pE-40}$ in the brain extracts of the mice. As shown in **Figure 2b**, among all the injected compounds, **212** exhibited significant $A\beta_{N3pE-40}$ lowering effects (54.7% inhibition), whereas compounds **1**, **170**

and **191** were found to be inactive via i.p. injection. A parallel artificial membrane permeability assay (PAMPA)[41] of these four compounds also correlated with the i.p. *in vivo* results, showing that **212** was the most permeable compound, while the other three compounds showed low permeabilities with similar –logPe values (**Table 4**). Additionally, we determined mouse liver microsomal stability of compound **212**, and found that percent remaining after 30 minutes was 50 percent, indicating that **212** is moderately stable for metabolism *in vivo*. These observations supported that a significant amount of **212** penetrated the BBB and successfully inhibited the brain QC.

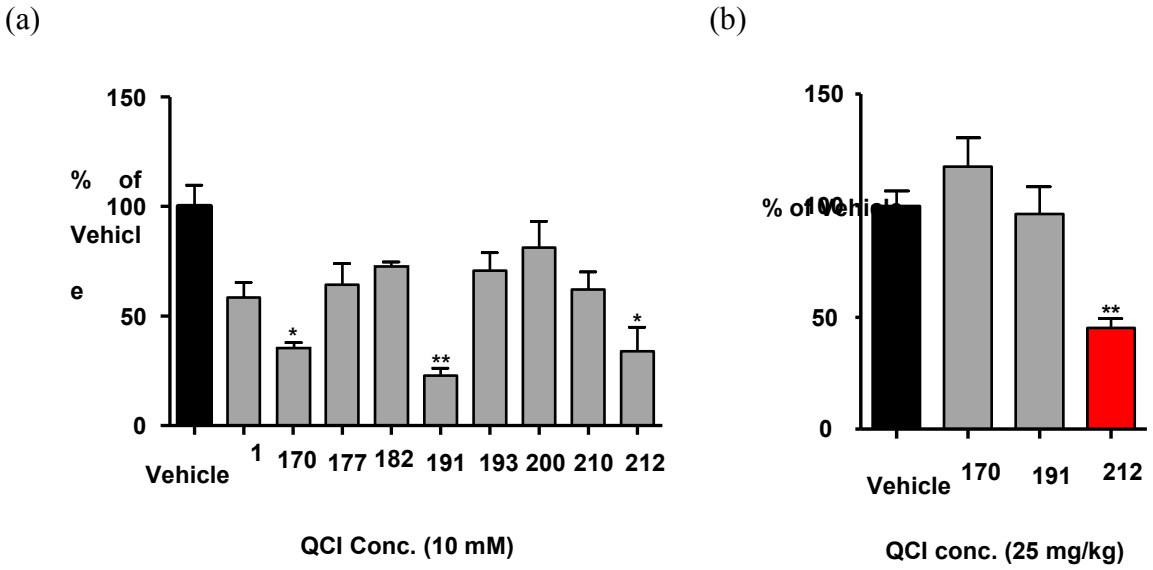

Figure 2. Inhibition of QC in acute AD model mice showing percent inhibition of the formation of human $A\beta_{N3pE-40}$ levels in brain after (a) deep cortical/hippocampus injection (10 mM); (b) i.p. injection of each inhibitor (25 mg/kg). Data were analyzed by One-way ANOVA with Bonferroni post-hoc test in SPSS. (*: $p < 0.05$, **: $p < 0.01$)

To validate the desired therapeutic effects of compound **212**, we next performed long-term studies in transgenic model mice of AD. **212** was administered to the APP/PS1 mice via deep cortical/hippocampus brain infusion for 21 days. After the brain infusion, the brain concentrations of $A\beta_{N3pE-42}$ and $A\beta_{1-42}$ were measured. As described in **Figure 3**, compound **212**

significantly reduced the brain concentrations of $A\beta_{N3pE-42}$ (**Figure 3a**), which corresponds to the observed percent inhibition in acute AD mice. Compound **212** also significantly reduced the total Aβ levels (**Figure 3b**) without significant toxicity, indicating that the inhibition of QC not only reduced the amount of pGlu-Aβ but also contributed to the overall reduction of amyloid formation.

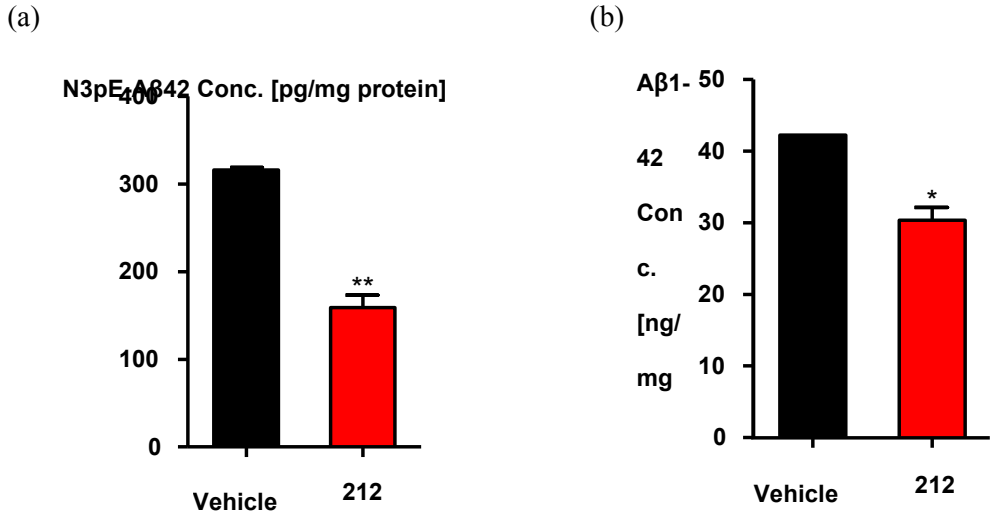

Figure 3. Inhibition of the formation of human $A\beta_{N3pE-42}$ and $A\beta_{1-42}$ in APP/PS1 mice. (a) Brain concentrations of $A\beta_{N3pE-42}$; (b) Brain concentrations of $A\beta_{1-42}$. Data were analyzed by unpaired t-test or one-way ANOVA. (ns: $p > 0.05$, *: $p < 0.05$, **: $p < 0.01$)

Next, we tested compound **212** in 5XFAD transgenic mice, a well-known AD mouse model suitable to study $A\beta_{42}$-induced neurodegeneration and amyloid plaque formation.[40] We specifically choose 5XFAD mice because this particular AD model generates severe AD related pathologies that were resulted from the massive increase of Aβ and the pyroform of Aβ in the brains.[25] $A\beta_{42}$ accumulates in the 5XFAD brain starting at 2 months of age, and develops other typical AD pathologies such as reduced synaptic markers, neuronal loss and memory impairments. We injected **212** into 5XFAD mice from 19 weeks to 34 weeks of age and performed the Morris Water Maze test to assess changes in the spatial memory impairment. The

efficacy of **212** in 5XFAD mice was evaluated based on the subsequent improvement in cognitive functions, as shown in **Figure 4**. The escape latency of **212**-treated mice became significantly shorter over repeated sessions compared with vehicle-treated mice (**Figure 4a**), indicating that the treatment of **212** improved cognitive function. Additionally, the duration of time spent in the target quadrant was significantly longer with **212** treated mice (**Figure 4b**), also supporting that the QC inhibitor **212** effectively recovered learning and memory function without fatal side effects.

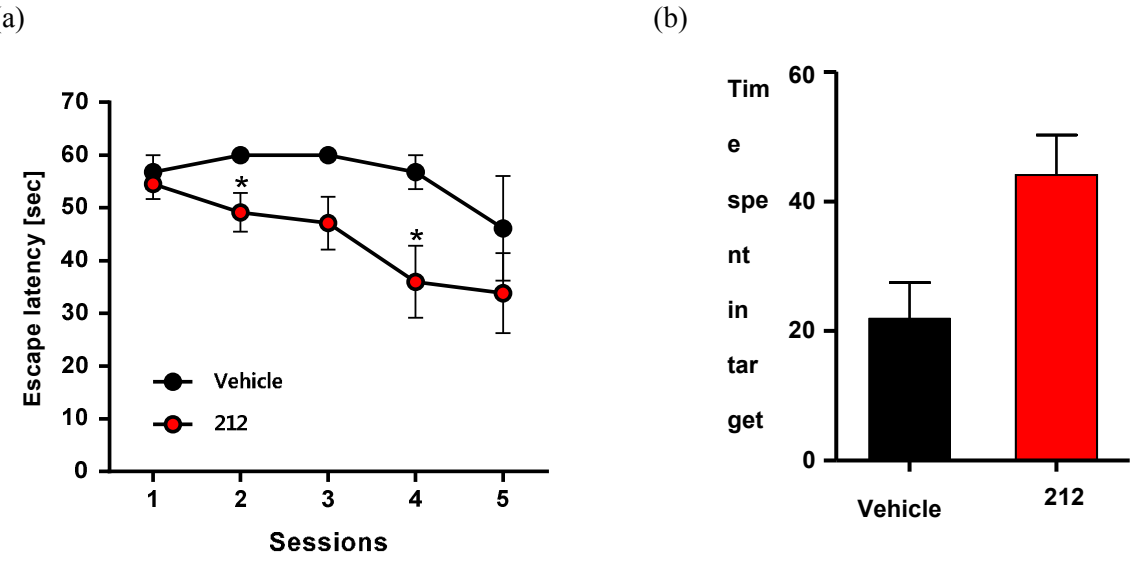

Figure 4. Effect of compound **212** on cognitive function of 5xFAD mice. (a) Escape latency of each group in the hidden-platform training of the Morris water maze. Data were analyzed by two-way repeated-measures ANOVA; (b) Percentage of time spent in the target quadrant. Data were analyzed by independent samples t-test in SPSS. (ns: $p > 0.05$, *: $p < 0.05$)

Molecular Modeling Studies.

Among the compounds we designed based on the *N*-terminal tripeptide (Glu-Phe-Arg) of $A\beta_{3E\text{-}42}$, compounds **191** and **212** exhibited excellent *in vitro* activity. Specifically, **191** demonstrated more than 40-fold higher potency compared with the reported dipeptide mimic compound **1**. Considering that the addition of the D-region pharmacophore improved the

inhibitory effects to such a great extent, we decided to study the mode of binding of these compounds in the *h*QC active site. For our docking studies, we utilized the X-ray crystal structure of *h*QC complexed with a known QC inhibitor, PBD150 (PDB id: 3PBB).[42] Since the ligand protonation states are important for an accurate docking study, we first performed the protonation state prediction of our ligands. At the physiological pH of 7.4, the D-region in **191** was monoprotonated in its major form and that of **212** was predicted to have neutral and protonated forms with the ratio of 2:1. Glide SP (Standard Precision) docking was also carried out, and both **191** and **212** docked very well into the active site of *h*QC. The 5-methyl imidazole in the A-region chelated with zinc and formed an H-bonding interaction with the indole NH of Trp329. Additionally, it displayed hydrophobic interactions with Leu249, Trp207, and Ile321. The thiourea group in the B-region acted as a linker, and the phenyl ring in the C-region exhibited a hydrophobic interaction with Tyr299. The piperazine or pyridine ring of the D-region also exhibited hydrophobic interactions with Pro326 and Pro324, but the NH in the Arg mimetic part of the compounds did not show any interactions. We further adopted Glide QM-Polarized Ligand Docking (QPLD) in Maestro, which can improve the docking accuracy over pure Molecular Mechanics (MM) methods by calculating the partial charges of the ligand using quantum mechanics (QM).[43] The resulting docking modes showed that the Arg mimetic D-region considerably moved toward the Glu327 of the hQC active site, denoting promising interactions between them. These encouraging results prompted us to further optimize the protein-ligand complexes.

The local optimization refinement made the side chain of Glu327 significantly move within the range of a salt bridge interaction with the D-region of our ligands. To estimate the global minimum, the protein-ligand complexes were further refined using Monte Carlo

minimization by randomly sampling the discrete set of energy minima and accumulating the energy contributions.[44] Finally, scrupulous optimization of the protein-ligand complexes produced a remarkable change in the position of the Glu327 side chain, allowing it to interact with the D-region of the ligands (Supporting Information).

For the most potent compound, **191**, the D-region displayed a salt bridge interaction as well as H-bonding with the side chain carboxylate of Glu327 (**Figure 5**). In the case of **212**, the D-region showed H-bonding interaction in its neutral form and a salt bridge interaction in its protonated form (**Figure 6**). In addition, the D-region of both compounds showed hydrophobic interactions with Pro326 and Val328. The A-region maintained docking results such as zinc chelation, H-bonding, and hydrophobic interactions. The thiourea group in the B-region formed an additional H-bonding with Gln304. The phenyl ring in the C-region presented π-π interactions with Phe325. Moreover, aside from the previous hydrophobic interaction with Tyr299, continuous refinements lead to the formation of additional hydrophobic interactions with Pro324 and Phe325.

In summary, our docking and refinement results showed that the designed and synthesized inhibitors bind very well in the active site of the hQC via the aggregated interactions of the A-, B-, C-, and D-regions. Notably, the Arg mimetic D-regions of the inhibitors were able to form strong interactions with the carboxylate group of Glu327, providing a feasible explanation of how our Arg mimetic compounds enhanced the inhibitory activity against *h*QC.

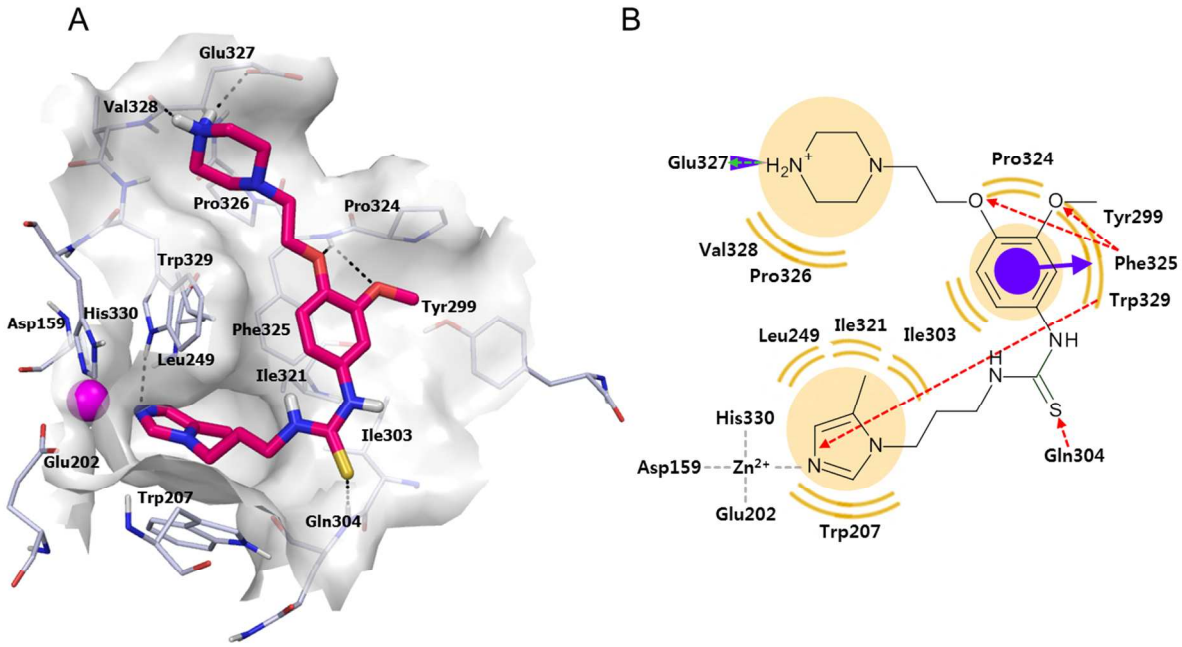

Figure 5. Docked and refined structure of **191** in hQC. (A) Binding interactions of **191** at the active site of hQC. **191** is displayed as sticks with magenta carbon atoms, and the Zn^{2+} is a purple ball. The interacted residues are depicted as light blue sticks. Hydrogen bonds are depicted as black dashed lines. (B) 2D representation of the interactions of **191** with the active site residues of the *h*QC. Hydrophobic interactions are marked in light brown. Hydrogen bonds are shown as red-dotted arrows with their directionality. The π-π stacking interaction is marked as a blue disc and arrow, and the salt bridge interaction is displayed as a blue wedge line.

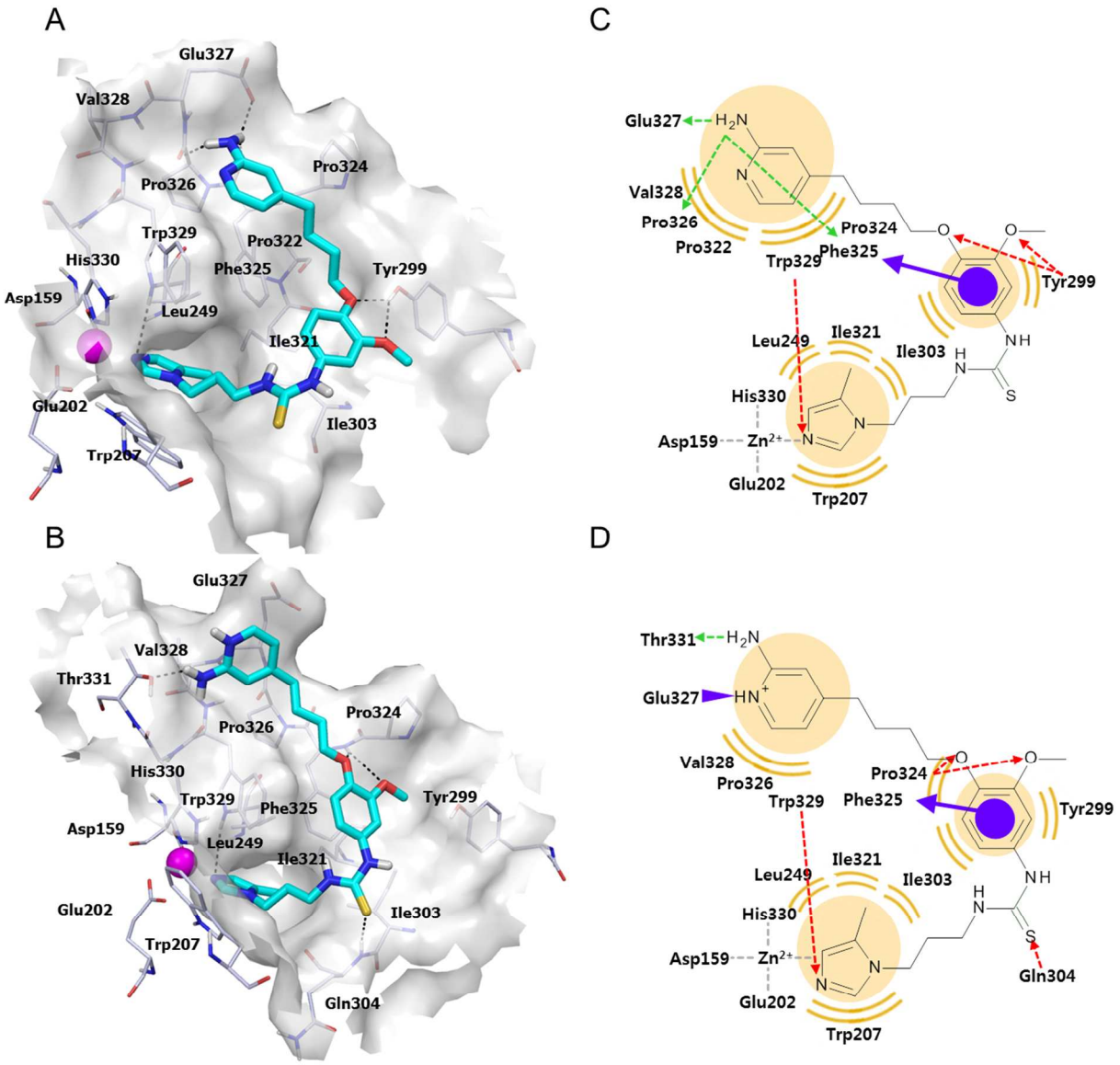

Figure 6. Docked and refined structures of **212** in hQC. Binding interactions of **212** in (A) neutral form and (B) protonated form at the active site of the hQC. **212** is represented in sticks with cyan carbon atoms, and Zn^{2+} is a purple ball. The interacted residues are depicted as light blue sticks. Hydrogen bonds are depicted as black dashed lines. 2D representation of **212** interactions in (C) neutral form and (D) protonated form with the active site of hQC. Hydrophobic interactions are marked in light brown. Hydrogen bonds are shown as red- and green-dotted arrows with their directionality. The π-π stacking interaction is marked as a blue disc and arrow, and the salt bridge interaction is displayed as a blue wedge line.

■ CONCLUSION

We developed novel QC inhibitors that have the potential to serve as a novel therapeutic option for AD. In particular, we aimed to further expand our library of QC inhibitors and designed compounds with an extended scaffold based on the *N*-terminal tripeptide (Glu-Phe-Arg) of $A\beta_{3E-42}$. In-depth SAR studies identified the eight most potent inhibitors, which demonstrated excellent QC inhibition, with from 5 to 40-fold increases in potency compared to a known inhibitor, compound **1**. These inhibitors were further tested in acute model mice for Aβ-lowering effects *in vivo*, and compound **212** penetrated the BBB and effectively reduced the brain levels of $A\beta_{1-42}$ and $A\beta_{N3pE-42}$. Moreover, we evaluated the *in vivo* efficacy of **212** in two different transgenic model mice of AD, APP/PS1 and 5xFAD, to verify the desired therapeutic effects. Compound **212** not only reduced the brain concentrations of pyroform Aβ and total Aβ in APP/PS1 mice but also restored cognitive functions in 5xFAD mice. This significant enhancement of the overall activity was achieved by adding the Arg mimetic D-region, which created an additional binding interaction. Stepwise computational studies utilizing quantum mechanics-based molecular docking and Monte Carlo algorithm-based refinement suggested that the Arg mimetic D-regions of **191** and **212** formed strong interactions with the carboxylate group of Glu327, and both compounds demonstrated favorable binding interactions with all four pharmacophoric regions. Taken together, compound **212** is an effective QC inhibitor for a possible therapeutic alternative in AD. We believe that this study provides useful insights in designing potent QC inhibitors in the future.

■ EXPERIMENTAL SECTION

General. All chemical reagents were commercially available. Melting points were determined on a melting point Buchi B-540 apparatus and are uncorrected. Silica gel column chromatography was performed on silica gel 60, 230–400 mesh, Merck. The PLC plates used PLC silica gel 60 F_{254}, 1 mm, Merck. ^{1}H and ^{13}C NMR spectra were recorded on a JEOL JNM-LA 300 at 300 MHz and 75 MHz, Bruker Analytik, DE/AVANCE Digital 400 at 400 MHz and 100 MHz, Bruker Analytik, DE/AVANCE Digital 500 at 500 MHz and 125 MHz, JEOL JNM-ECA-600 at 600 MHz and 150 MHz, Ultrashielded Bruker Avance III HD NMR spectrometer at 800 MHz and 200 MHz, respectively. Chemical shifts are reported in ppm units with Me_4Si as a reference standard. Mass spectra were recorded on a VG Trio-2 GC−MS instrument and a 6460 Triple Quad LC−MS instrument. All final compounds were purified to > 95% purity, as determined by high-performance liquid chromatography (HPLC). HPLC was performed on an Agilent 1120 Compact LC (G4288A) instrument using an Agilent TC-C18 column (4.6 mm × 250 mm, 5 μm).

General procedure for C-alkylated reaction (Procedure 1). A solution of a picoline derivative (1 equiv) in anhydrous THF was added dropwise to an *n*-butyllithium solution 2.5 M in THF (1.5 equiv for compounds **85** and **86**; 2.5 equiv for compounds **87-89**, **92**; 3.5 equiv for **93**) at -78°C under nitrogen. The reaction mixture was stirred at room temperature for 30 minutes before being cooled again to -78°C. 1-Bromo-2-chloroethane (1.1 equiv, compounds **85, 87**), 1-bromo-3-chloropropane (1.1 equiv, compound **86**), (3-bromopropoxy)-(*tert*-butyl)dimethylsilane (1.1 equiv, compounds **88, 89**) or diethyl carbonate (1.5 equiv, compounds **92, 93**) in anhydrous THF was added slowly to the reaction mixture. The reaction was monitored by TLC, and water was added when the reaction was finished. The mixture was extracted by EtOAc, washed by water,

dried over $MgSO_4$, and concentrated. The product was purified by silica gel chromatography with a gradient of 10 to 25% EtOAc in *n*-hexane as the eluting solvent.

General procedure for Williamson reaction (Procedure 2). To a suspension of 4-nitroguaiacol **2** (1.0 equiv) and potassium carbonate (compounds **3-5, 25-30, 96-98**) or cesium carbonate (compound **74**) (2.0 equiv) in anhydrous DMF, an alkyl halide was added. The reaction mixture was heated to 100°C for 1 hour and then cooled to room temperature and quenched by the addition of water. The precipitated was formed, filtered, and washed with water (3 times). The yellow solid product was collected, dried under vacuum and carried on to the next step without further purification or the crude was purified by column chromatography.

General procedure for *N*-alkylation (Procedure 3). To a solution of an amine (1.5 equiv) and the same amine participating in the reaction (2.0 equiv) as a base (compounds **6-17**) in anhydrous DMF, alkyl halide (1.0 equiv) was added. The reaction mixture was heated to 60°C until the starting material was consumed, and then it was cooled to room temperature and quenched by the addition of water. The precipitate was formed, filtered, and washed with water (3 times) and the solid product was collected, dried under vacuum and carried on to the next step without further purification; or the crude was purified by column chromatography.

General procedure for the reduction of the nitro group to an amine group or alkyne derivatives to alkyl derivatives (Procedure 4). The nitro compound or the alkyne compound was dissolved in MeOH (or a mixture of MeOH and THF), and then 10% Pd/C was added. The mixture was stirred at room temperature under hydrogen gas until the starting material was consumed. The crude mixture was filtered through Celite, washed with methanol, and then

concentrated. The product was carried on to the next step without further purification or was purified by column chromatography.

General procedure for thiourea coupling (**Procedure 5)**. To a solution of 1,1'-thiocarbonyldiimidazole (TCDI) (1.02 equiv) in anhydrous DCM was added dropwise a solution of arylamine (1.0 equiv) in anhydrous DCM under nitrogen gas at room temperature. The reaction mixture was stirred at room temperature until the starting material was consumed, and then a solution of 3-(5-methyl-1*H*-imidazol-1-yl)propan-1-amine (1.1 equiv) in anhydrous DCM was added dropwise, followed by the addition of triethylamine (3.0 equiv) and stirring at room temperature until the reaction was complete (as monitored by TLC). The mixture was washed 2 times by water. The combined organic layer was dried over $MgSO_4$, concentrated, and purified by column chromatography.

General procedure for Boc-protection (Procedure 6). To a suspension of starting material amine (1.0 equiv) in DCM or *tert*-butyl alcohol (compounds **83, 84**) was added triethylamine (1.2 equiv) and di-*tert*-butyl dicarbonate in DCM under ice cooling. The mixture was stirred at room temperature until the staring material was consumed. To this was added water, and it was extracted with DCM. The organic layer was washed with 10% aqueous $NaHCO_3$ solution, water, and brine, dried over $MgSO_4$, filtered, and concentrated in vacuo. The residue was purified by column chromatography.

General procedure for Boc-deprotection (Procedure 7). Trifluoroacetic acid (10.0 equiv) was added to the solution of *boc*-protected compound (1.0 equiv) in DCM (DCM:TFA = 1:1 (v/v)). The mixture was stirred at room temperature until the starting material was consumed, and then

the solvent was evaporated. The residue was dissolved in MeOH and purified by an ion-exchange column or water was added to the residue, and then it was basified by 1 N NaOH and extracted by DCM (2 times). The combined organic layer was washed with brine, dried over $MgSO_4$, and purified by PLC or column chromatography to give the desired product.

General procedure for Mitsunobu reaction (Procedure 8). Triphenylphosphine (1.3 equiv) was added under nitrogen to a solution of 4-nitroguaiacol (**2**) (1.0 equiv) in DCM, followed by the addition of a primary alcohol (1.2 equiv) and a solution of diethyl azodicarboxylate (1.3 equiv) in DCM (2 mL). After the solution was stirred for 30 minutes at ambient temperature, the reaction mixture was poured onto a column of silica and was eluted with EtOAc/*n*-hexane to give the desired product.

General procedure for Sonogashira coupling reaction (Procedure 9). To a 3-necked round bottom flask of a solution of aryl halide (1.0 equiv) in anhydrous DCM was added copper iodide (5% mol), tetrakis(triphenylphosphine)palladium (0) (5% mol), triethylamine (3.0 equiv) and a terminal alkyne (2.0 equiv) under argon, and the reaction was stirred at 50°C for 15 hours. The reaction was diluted with EtOAc and washed with saturated aqueous NH_4Cl solution (twice), and the combined aqueous layers were extracted with EtOAc (3 times). The combined organic layers were washed with brine, dried over $MgSO_4$ and concentrated. Column chromatography (*n*-hexane:EtOAc) yielded the desired product.

1-(4-(2-Aminoethoxy)-3-methoxyphenyl)-3-(3-(5-methyl-1*H*-imidazol-1-yl)propyl)thiourea (169). From compound **146**, procedure **7**. yield 54%, white solid, mp 84-85 ^{o}C. ^{1}H NMR (300 MHz, CD_3OD) δ 7.59 (d, J = 1.11 Hz, 1H), 6.98 (d, J = 8.61 Hz, 1H), 6.94 (d, J = 2.22 Hz, 1H),

6.78 (dd, J = 8.43, 2.40 Hz, 1H), 6.66 (s, 1H), 4.04 (t, J = 5.31 Hz, 2H), 3.99 (t, J = 7.32 Hz, 2H), 3.83 (s, 3H), 3.61 (t, J = 6.96 Hz, 2H), 3.00 (t, J = 5.31 Hz, 2H), 2.22 (d, J = 0.93 Hz, 3H), 2.07 (quintet, J = 7.14 Hz, 2H). ^{13}C NMR (200 MHz, CD_3OD) δ 183.3, 152.0, 148.6, 138.8, 133.8, 129.8, 127.3, 119.9, 116.3, 112.0, 71.8, 57.3, 44.1, 43.8, 42.3, 32.0, 9.9. MS(FAB) *m/z* 364 $[M+H]^+$. HRMS (FAB) calc. for $C_{17}H_{25}N_5O_2S$ $[M + H]^+$ 364.1807, found 364.1805.

1-(4-(3-Aminopropoxy)-3-methoxyphenyl)-3-(3-(5-methyl-1*H*-imidazol-1-yl)propyl)-thiourea (170). Compound **167** (1.0 equiv) was dissolved in ethanol and hydrazine monohydrate (5.0 equiv) was added dropwise. The mixture was stirred at room temperature until the starting material consumed. The formed precipitate was filtered off and washed with ethanol. The filtrate was collected and concentrated by rotary evaporation to afford the desired product as an off white solid (48 mg, 42%), mp 78-79 ^{o}C. ^{1}H NMR (300 MHz, CD_3OD) δ 7.59 (s, 1H), 6.97 (d, J = 8.61 Hz, 1H), 6.91 (d, J = 2.19 Hz, 1H), 6.77 (dd, J = 8.43, 2.37 Hz, 1H), 6.66 (s, 1H), 4.09 (t, J = 6.06 Hz, 2H), 4.00 (t, J = 6.96 Hz, 2H), 3.81 (s, 3H), 3.62 (t, J = 6.57 Hz, 2H), 2.86 (t, J = 6.78 Hz, 2H), 2.22 (d, J = 0.93 Hz, 3H), 2.08 (quintet, J = 7.14 Hz, 2H), 1.96 (quintet, J = 6.24 Hz, 2H). ^{13}C NMR (200 MHz, CD_3OD) δ 183.4, 151.9, 148.6, 138.7, 133.4, 129.8, 127.3, 119.9, 116.4, 112.0, 70.1, 57.2, 44.1, 43.8, 42.0, 32.0, 27.5, 9.9. MS(FAB) *m/z* 378 $[M+H]^+$. HRMS (FAB) calc. for $C_{18}H_{27}N_5O_2S$ $[M + H]^+$ 378.1958, found 378.1965.

1-(4-(4-Aminobutoxy)-3-methoxyphenyl)-3-(3-(5-methyl-1*H*-imidazol-1-yl)propyl)-thiourea (171). Prepared from compound **168** by following the experiment procedure used for compound **170** to afford the desired product as a white solid (38 mg, 40%), the compound was decomposed at 199 ^{o}C. ^{1}H NMR (300 MHz, CD_3OD) δ 7.59 (d, J = 0.93 Hz, 1H), 6.95-6.92 (m, 2H), 6.77 (dd,

J = 8.40, 2.37 Hz, 1H), 6.66 (s, 1H), 4.03-3.95 (m, 4H), 3.81 (s, 3H), 3.61 (t, *J* = 5.67 Hz, 2H), 2.82 (t, *J* = 7.14 Hz, 2H), 2.22 (d, *J* = 0.93 Hz, 3H), 2.07 (quintet, *J* = 7.14 Hz, 2H), 1.88 (quintet, *J* = 6.24 Hz, 2H), 1.76 (quintet, *J* = 6.75 Hz, 2H). ^{13}C NMR (200 MHz, CD_3OD) δ 183.5, 151.9, 148.7, 138.8, 133.6, 129.8, 127.3, 119.7, 115.5, 112.0, 70.7, 57.3, 44.2, 43.8, 41.6, 32.1, 28.0, 26.9, 9.9. MS(FAB) *m/z* 392 $[M+H]^+$. HRMS (FAB) calc. for $C_{19}H_{29}N_5O_2S$ $[M + H]^+$ 392.2120, found 392.2112.

1-(3-Methoxy-4-(2-(methylamino)ethoxy)phenyl)-3-(3-(5-methyl-1*H*-imidazol-1-yl)propyl)thiourea (172). From compound **149**, procedure **7**. yield 34%, white solid, mp 73-74 ^{o}C. ^{1}H NMR (300 MHz, CD_3OD) δ 7.60 (s, 1H), 6.98 (d, *J* = 8.40 Hz, 1H), 6.97 (s, 1H), 6.77 (dd, *J* = 8.16, 2.37 Hz, 1H), 6.67 (s, 1H), 4.12 (t, *J* = 5.13 Hz, 2H), 3.98 (t, *J* = 7.32 Hz, 2H), 3.83 (s, 3H), 3.57 (t, *J* = 6.42 Hz, 2H), 3.00 (t, *J* = 5.31 Hz, 2H), 2.50 (s, 3H), 2.22 (d, *J* = 0.9 Hz, 3H), 2.04 (quintet, *J* = 6.75 Hz, 2H). MS(ESI) *m/z* 378 $[M+H]^+$. ^{13}C NMR (200 MHz, CD_3OD) δ 183.3, 152.0, 148.6, 138.8, 133.8, 129.7, 127.3, 119.8, 116.4, 112.1, 69.6, 57.3, 51.7, 44.1, 43.8, 36.3, 32.0, 9.9. HRMS (FAB) calc. for $C_{18}H_{27}N_5O_2S$ $[M + H]^+$ 378.1963, found 378.1954.

1-(3-Methoxy-4-(3-(methylamino)propoxy)phenyl)-3-(3-(5-methyl-1*H*-imidazol-1-yl)propyl) thiourea (173). From compound **150**, procedure **7**. yield 74%, white solid, mp 80-81 ^{o}C. ^{1}H NMR (300 MHz, CD_3OD) δ 7.59 (d, *J* = 1.11 Hz, 1H), 6.95 (d, *J* = 8.61 Hz, 1H), 6.93 (d, *J* = 2.37 Hz, 1H), 6.75 (dd, *J* = 8.31, 2.37 Hz, 1H), 6.66 (s, 1H), 4.08 (t, *J* = 6.06 Hz, 2H), 3.97 (t, *J* = 7.32 Hz, 2H), 3.82 (s, 3H), 3.95 (t, *J* = 6.42 Hz, 2H), 2.84 (t, *J* = 6.75 Hz, 2H), 2.46 (s, 3H), 2.22 (d, *J* = 0.93 Hz, 3H), 2.08 - 1.97 (m, 4H). ^{13}C NMR (125 MHz, $CDCl_3$) δ 181.3, 149.8, 146.9, 136.3, 129.9, 127.2, 125.9, 118.0, 113.4, 109.9, 67.7, 55.8, 48.5, 42.2, 41.8, 35.0, 29.9, 27.6, 9.2.

MS (FAB) m/z 392 $[M+H]^+$. HRMS (FAB) calcd for $C_{19}H_{29}N_5O_2S$ ($M + H^+$) 392.2115 , found 392.2135.

1-(3-Methoxy-4-(3-(methylamino)butoxy)phenyl)-3-(3-(5-methyl-1*H*-imidazol-1-yl)propyl)thiourea (174). From compound **151**, procedure **7**, yield 31%, white solid, mp 60-61 ^oC. ^1H NMR (300 MHz, CD_3OD) δ 7.59 (d, J = 1.08 Hz, 1H), 6.93 (d, J = 8.61 Hz, 1H), 6.92 (d, J = 2.73 Hz, 1H), 6.75 (dd, J = 8.61, 2.55 Hz, 1H), 6.66 (s, 1H), 4.02 (t, J = 5.67 Hz, 2H), 3.95 (t, J = 7.32 Hz, 2H), 3.81 (s, 3H), 3.59 (t, J = 6.78 Hz, 2H), 2.76 (t, J = 7.2 Hz, 2H), 2.47 (s, 3H), 2.22 (d, J = 0.93 Hz, 3H), 2.03 (quintet, J = 6.95 Hz, 2H), 1.87-1.73 (m, 4H). ^{13}C NMR (200 MHz, CD_3OD) δ 183.3, 151.8, 148.9, 138.7, 133.2, 129.7, 127.3, 119.8, 115.5, 112.1, 70.8, 57.3, 52.1, 44.1, 43.8, 35.6, 32.1, 28.3, 26.5, 9.9. MS (ESI) m/z 406 $[M+H]^+$. HRMS (FAB) calcd for $C_{20}H_{31}N_5O_2S$ $[M+H]^+$ 406.2276, found 406.2270.

1-(4-(2-(Dimethylamino)ethoxy)-3-methoxyphenyl)-3-(3-(5-methyl-1*H*-imidazol-1-yl)propyl)thiourea (175). From compound **103**, procedure **5**, yield 50%, off white solid, mp 153-154 ^oC. ^1H NMR (300 MHz, CD_3OD) δ 7.62 (s, 1H), 6.99 (d, J = 8.61 Hz, 1H), 6.96 (d, J = 3.27 Hz, 1H), 6.78 (dd, J = 8.43, 2.40 Hz, 1H), 6.67 (s, 1H), 4.15 (t, J = 5.49 Hz, 2H), 4.00 (t, J = 7.14 Hz, 2H), 3.81 (s, 3H), 3.61 (t, J = 6.57 Hz, 2H), 2.92 (t, J = 5.49 Hz, 2H), 2.46 (s, 6H), 2.22 (d, J = 1.08 Hz, 3H), 2.08 (quintet, J = 7.32 Hz, 2H). ^{13}C NMR (200 MHz, CD_3OD) δ 183.5, 152.5, 148.3, 138.8, 134.4, 129.9, 127.1, 119.5, 117.2, 112.0, 68.4, 59.5, 57.2, 46.1, 44.3, 43.7, 32.1, 9.9. MS (FAB) *m/z* 392 $[M+H]^+$. HRMS (FAB) calc. for $C_{19}H_{29}N_5O_2S$ $[M + H]^+$ 392.2120 found, 392.2128.

1-(4-(3-(Dimethylamino)propoxy)-3-methoxyphenyl)-3-(3-(5-methyl-1*H*-imidazol-1-yl)propyl)thiourea (176). From compound **104**, procedure **5**. yield 50%, off white solid, the compound was decomposed at 195 ^{o}C. ^{1}H NMR (300 MHz, CD_3OD) δ 7.62 (s, 1H), 6.97 (s, 1H), 6.95 (s, 1H), 6.79 (dd, J = 8.61, 2.37 Hz, 1H), 6.68 (s, 1H), 4.11 (t, J = 5.88 Hz, 2H), 4.01 (t, J = 7.14 Hz, 2H), 3.83 (s, 3H), 3.60 (t, J = 6.96 Hz, 2H), 3.02 (t, J = 7.32 Hz, 2H), 2.65 (s, 6H), 2.23 (d, J = 0.90 Hz, 3H), 2.15-2.02 (m, 4H). ^{13}C NMR (125 MHz, CD_3OD) δ 183.5, 152.0, 148.5, 138.7, 134.1, 129.9, 127.1, 119.6, 116.2, 112.0, 69.4, 58.4, 57.4, 45.1, 44.3, 43.7, 32.1, 27.2, 9.9. MS (FAB) *m/z* 406 $[M+H]^+$. HRMS (FAB) calc. for $C_{20}H_{31}N_5O_2S$ $[M + H]^+$ 406.2271, found 406.2277.

1-(4-(4-(Dimethylamino)butoxy)-3-methoxyphenyl)-3-(3-(5-methyl-1*H*-imidazol-1-yl)propyl)thiourea (177). From compound **105**, procedure **5**. yield 87%, white solid, mp 50-51 ^{o}C. ^{1}H NMR (300 MHz, $CDCl_3$) δ 7.60 (s, 1H), 7.37 (s, 1H), 6.87 (d, J = 8.25 Hz, 1H), 6.75 - 6.70 (m, 3H), 5.95 (s, 1H), 4.05 (t, J = 6.42 Hz, 2H), 3.89 (t, J = 6.96 Hz, 2H), 3.83 (s, 3H), 3.66 (q, J = 7.32 Hz, 2H), 2.36 (t, J = 7.5 Hz, 2H), 2.25 (s, 6H), 2.17 (d, J = 0.93 Hz, 3H), 2.05 (t, J = 7.14 Hz, 2H), 1.89-1.86 (m, 2H), 1.67 (quintet, J = 6.78 Hz, 2H). ^{13}C NMR (75 MHz, CD_3OD) δ 183.3, 152.2, 149.3, 138.8, 133.1, 129.7, 127.4, 119.8, 115.9, 112.2, 71.0, 61.1, 57.3, 46.0, 44.2, 43.8, 32.2, 29.0, 25.6, 9.9. MS (ESI) *m/z* 420 $[M+H]^+$. HRMS (FAB) calc. for $C_{21}H_{33}N_5O_2S$ $[M + H]^+$ 420.2428, found 420.2430.

***N*-(3-(2-Methoxy-4-(3-(3-(5-methyl-1*H*-imidazol-1-yl)propyl)thioureido)phenoxy)propyl)acetamide (178)**. Prepared from compound **170** (100 mg, 1.0 equiv) was dissolved in solution of pyridine (3 equiv) in DCM (10 mL) then acetic anhydride

(1.1 equiv) was added to the mixture. The mixture reaction was stirred room temperature for 4 hours, and diluted with DCM, then washed with water, dried over $MgSO_4$ and purified by silica gel chromatography to afford the desired product as a white solid (86 mg, 77%), mp 125-126 ^oC. ^1H NMR (300 MHz, $CDCl_3$) δ 7.65 (s, 1H), 7.32 (s, 1H), 6.87 (d, J = 8.97 Hz, 1H), 6.76 - 6.71 (m, 4H), 5.96 (s, 1H), 4.14 (t, J = 5.67 Hz, 2H), 3.90 (t, J = 6.96 Hz, 2H), 3.86 (s, 3H), 3.62 (q, J = 6.96 Hz, 2H), 3.48 (q, J = 5.49 Hz, 2H), 2.19 (s, 3H), 2.11-1.97 (m, 4H), 1.99 (s, 3H). ^{13}C NMR (200 MHz, $CDCl_3$) δ 181.8, 170.1, 149.8, 147.1, 136.5, 129.7, 127.1, 126.5, 118.2, 112.8, 109.9, 68.5, 55.9, 42.3, 42.1, 37.9, 30.1, 28.5, 23.2, 9.2. MS (FAB) *m/z* 420 $[M+H]^+$. HRMS (FAB) calc. for $C_{20}H_{29}N_5O_3S$ $[M+H]^+$ 420.2064, found 420.2060.

1-(4-(3-Guanidinopropoxy)-3-methoxyphenyl)-3-(3-(5-methyl-1*H*-imidazol-1-yl)propyl)-thiourea (179). To compound **170** (50 mg, 0.13 mmol) and 1*H*-pyrazole-1-carboxamidine hydrochloride (78 mg, 0.53 mmol) in anhydrous methanol (2 mL) was added diisopropylethylamine (0.23 mL, 1.3 mmol), and the reaction mixture was stirred at 50 ^oC for 12 hours. The resulting mixture was purified by PLC (MeOH/DCM = 2/9) to afford the product as a white solid (25 mg, 46%), mp 256-257 ^oC. ^1H NMR (300 MHz, CD_3OD) δ 7.51 (s, 1H), 6.92 (d, J = 2.19 Hz, 1H), 6.89 - 6.84 (m, 1H), 6.69 (dd, J = 6.57, 2.37 Hz, 1H), 6.57 (s, 1H), 4.01 (t, J = 5.85 Hz, 2H), 3. 92 (t, J = 7.14 Hz, 2H), 3.74 (s, 3H), 3.50 (t, J = 6.03 Hz, 2H), 3.33 (t, J = 6.60 Hz, 2H), 2.13 (d, J = 0.93 Hz, 3H), 2.00-1.93 (m, 4H). ^{13}C NMR (200 MHz, CD_3OD) δ 183.4, 157.7, 152.0, 148.4, 138.7, 133.8, 129.6, 127.3, 119.5, 117.4, 112.1, 69.4, 57.5, 44.2, 43.5, 40.1, 32.2, 25.2, 9.9. MS (FAB) *m/z* 420 $[M+H]^+$. HRMS (FAB) calc. for $C_{19}H_{29}N_7O_2S$ $[M + H]^+$ 420.2176, found 420.2191.

1-(3-Methoxy-4-(2-(pyrimidin-2-ylamino)ethoxy)phenyl)-3-(3-(5-methyl-1*H*-imidazol-1-yl)propyl)thiourea (180). Compound **169** (98 mg, 0.27 mmol) was dissolved in ethanol. 2-Chloropyrimidine (78 mg, 0.54 mmol) and 0.7 mL of triethylamine were added. The mixture was refluxed for 2 days, then solvent was removed by rotary evaporation, purified by PLC (MeOH/DCM = 1/9) to give a yellow solid product (85 mg, 72%), mp 83-84 ^{o}C. ^{1}H NMR (300 MHz, CD_3OD) δ 8.27 (d, J = 4.95 Hz, 2H), 7.72 (s, 1H), 7.00 (d, J = 8.43 Hz, 1H), 6.92 (d, J = 2.19 Hz, 1H), 6.76-6.72 (m, 2H), 6.62 (t, J = 4.74 Hz, 1H), 4.15 (t, J = 5.49 Hz, 2H), 4.01 (t, J = 7.32 Hz, 2H), 3.81 (s, 3H), 3.77 (t, J = 5.49 Hz, 2H), 3.61 (t, J = 6.96 Hz, 2H), 2.22 (d, J = 0.9 Hz, 3H), 2.08 (quintet, J = 6.96 Hz, 2H). ^{13}C NMR (200 MHz, CD_3OD) δ 183.4, 164.3, 160.1, 152.2, 148.9, 138.6, 133.6, 130.1, 126.5, 119.8, 116.4, 112.4, 112.2, 70.2, 57.4, 44.4, 43.7, 42.5, 32.1, 9.9. MS (FAB) *m/z* 442 $[M+H]^+$. HRMS (FAB) calc. for $C_{21}H_{27}N_7O_2S$ $[M + H]^+$ 442.2025, found 442.2036.

1-(3-Methoxy-4-(3-(pyrimidin-2-ylamino)propoxy)phenyl)-3-(3-(5-methyl-1*H*-imidazol-1-yl)propyl)thiourea (181). Prepared from compound **170** (230 mg, 0.61 mmol) and 2-chloropyrimidine (140 mg, 1.22 mmol) by following the experiment procedure used for compound **180** to afford a yellow solid product (90 mg, 64%), mp 86-87 ^{o}C. ^{1}H NMR (300 MHz, CD_3OD) δ 8.25 (d, J = 4.77 Hz, 2H), 7.59 (s, 1H), 6.97 (d, J = 8.61 Hz, 1H), 6.91 (d, J = 2.19 Hz, 1H), 6.76 (dd, J = 8.43, 2.40 Hz, 1H), 6.66 (s, 1H), 6.59 (t, J = 4.95, 1H), 4.12 (t, J = 6.06 Hz, 2H), 3.99 (t, J = 7.14 Hz, 2H), 3.83 (s, 3H), 3,62-3.53 (m, 4H), 2.22 (d, J = 0.93 Hz, 3H), 2.11-2.01 (m, 4H). ^{13}C NMR (75 MHz, CD_3OD) δ 183.3, 164.3, 160.1, 152.2, 149.1, 138.8, 133.2, 129.7, 127.3, 119.7, 116.0, 112.1, 112.0, 69.6, 57.3, 44.2, 43.8, 40.4, 32.2, 25.0, 9.9. MS (FAB) *m/z* 456 $[M+H]^+$. HRMS (FAB) calc. for $C_{22}H_{29}N_7O_2S$ $[M + H]^+$ 456.2176, found 456.2182.

1-(3-Methoxy-4-(4-(pyrimidin-2-ylamino)butoxy)phenyl)-3-(3-(5-methyl-1*H*-imidazol-1-yl)propyl)thiourea (182). Prepared from compound **171** (300 mg, 0.77 mmol) and 2-chloropyrimidine (176 mg, 1.53 mmol) by following the experiment procedure used for compound **180** to afford a white solid product (129 mg, 36%), mp 175-176 ^{o}C. ^{1}H NMR (300 MHz, CD_3OD) δ 8.12 (d, J = 4.95 Hz, 2H), 7.48 (d, J = 2.52 Hz, 1H), 6.79 (d, J = 1.29 Hz, 1H), 6.78 (s, 1H), 6.66 (dd, J = 8.61, 2.37 Hz, 1H), 6.55 (s, 1H), 6.45 (t, J = 4.77 Hz, 1H), 3.91 (t, J = 5.85 Hz, 2H), 3.87 (t, J = 7.5 Hz, 2H), 3.67 (s, 3H), 3.48 (t, J = 6.95 Hz, 2H), 3.28 (t, J = 6.60 Hz, 2H), 2.09 (d, J = 0.90 Hz, 3H), 1.96 (quintet, J = 7.14 Hz, 2H), 1.75-1.60 (m, 4H). ^{13}C NMR (200 MHz, CD_3OD) δ 183.3, 164.3, 160.0, 152.1, 149.3, 138.8, 130.1, 129.7, 127.3, 119.8, 115.7, 112.1, 111.8, 71.0, 57.3, 44.2, 43.8, 42.6, 32.2, 28.4, 27.9, 9.9. MS (FAB) *m/z* 470 $[M+H]^+$. HRMS (FAB) calc. for $C_{23}H_{31}N_7O_2S$ $[M + H]^+$ 470.2338, found 470.2338.

1-(4-(3-(5-Fluoropyrimidin-2-ylamino)propoxy)-3-methoxyphenyl)-3-(3-(5-methyl-1*H*-imidazol-1-yl)propyl)thiourea (183). Prepared from compound **170** (150 mg, 0.40 mmol) and 2-chloro-5-fluoropyrimidine (0.098 mL, 0.80 mmol) by following the experiment procedure used for compound **180** to afford an off white solid product (65 mg, 65%), mp 75-76 ^{o}C. ^{1}H NMR (300 MHz, CD_3OD) δ 8.20 (d, J = 0.75 Hz, 2H), 7.59 (s, 1H), 6.96 (d, J = 8.43 Hz, 1H), 6.90 (d, J = 2.19 Hz, 1H), 6.75 (dd, J = 8.61, 2.37 Hz, 1H), 6.66 (s, 1H), 4.11 (t, J = 6.06 Hz, 2H), 3.97 (t, J = 7.14 Hz, 2H), 3.70 (s, 3H), 3.61 (t, J = 7.35 Hz, 2H), 3.54 (t, J = 6.42 Hz, 2H), 2.21 (d, J = 0.72 Hz, 3H), 2.09-2.00 (m, 4H). ^{13}C NMR (75 MHz, CD_3OD) δ 183.2, 161.8, 154.0 (d, $^{2}J_{C\text{-}F}$ = 243 Hz), 152.1, 149.1, 147.3 (d, $^{3}J_{C\text{-}F}$ = 22 Hz), 138.7, 133.1, 129.7, 127.3, 119.7, 115.8, 112.0, 69.6, 57.3, 44.2, 43.8, 41.0, 32.2, 30.8, 9.9. MS (FAB) *m/z* 474 $[M+H]^+$. HRMS (FAB) calc. for $C_{22}H_{28}FN_7O_2S$ $[M + H]^+$ 474.2087, found 474.2086.

1-(4-(4-(5-Fluoropyrimidin-2-ylamino)butoxy)-3-methoxyphenyl)-3-(3-(5-methyl-1*H*-imidazol-1-yl)propyl)thiourea (184). Prepared from compound **171** (100 mg, 0.26 mmol) and 2-chloro-5-fluoropyrimidine (0.063 mL, 0.51 mmol) by following the procedure described for compound **180** to afford a yellow solid product (53 mg, 42%), mp 70-71 ^{o}C. ^{1}H NMR (300 MHz, CD_3OD) δ 8.09 (d, J = 1.08 Hz, 2H), 7.49 (d, J = 0.93 Hz, 1H), 6.84 (d, J = 8.61 Hz, 1H), 6.80 (s, 1H), 6.66 (dd, J = 8.43, 2.37 Hz, 1H), 6.56 (s, 1H), 3.93 (t, J = 5.85 Hz, 2H), 3.86 (t, J = 7.14 Hz, 2H), 3.70 (s, 3H), 3.51 (t, J = 6.78 Hz, 2H), 3.31 (t, J = 6.75 Hz, 2H), 2.11 (d, J = 0.90 Hz, 3H), 1.97 (quintet, J = 7.14 Hz, 2H), 1.74-1.61 (m, 4H). ^{13}C NMR (200 MHz, CD_3OD) δ 183.3, 161.9, 153.9 (d, $^{2}J_{C\text{-}F}$ = 243 Hz), 152.1, 149.3, 147.3 (d, $^{3}J_{C\text{-}F}$ = 20 Hz) 138.8, 130.0, 129.7, 127.3, 119.8, 115.7, 112.1, 71.0, 57.3, 44.2, 43.8, 43.1, 32.2, 28.5, 27.9, 9.9. MS (FAB) *m/z* 488 $[M+H]^+$. HRMS (FAB) calc. for $C_{23}H_{30}FN_7O_2S$ $[M + H]^+$ 488.2244, found 488.2244.

1-(3-Methoxy-4-(2-(piperidin-1-yl)ethoxy)phenyl)-3-(3-(5-methyl-1*H*-imidazol-1-yl)propyl)thiourea (185). From compound **106**, procedure **5**. yield 59%, white solid, mp 100-101 ^{o}C. ^{1}H NMR (300 MHz, CD_3OD) δ 7.50 (d, J = 0.75 Hz, 1H), 6.87 (d, J = 5.85 Hz, 1H), 6.84 (s, 1H), 6.68 (dd, J = 8.49, 2.19 Hz, 1H), 6.56 (s, 1H), 4.05 (t, J = 5.70 Hz, 2H), 3.90 (t, J = 6.96 Hz, 2H), 3.70 (s, 3H), 3.51 (t, J = 6.75 Hz, 2H), 2.69 (t, J = 5.67 Hz, 2H), 2.46 (br, 4H), 2.12 (d, J = 0.75 Hz, 3H), 1.98 (quintet, J = 7.14 Hz, 2H), 1.55 - 1.48 (m, 4H), 1.39-1.37 (m, 2H). ^{13}C NMR (200 MHz, CD_3OD) δ 183.4, 152.3, 148.7, 138.8, 133.9, 129.7, 127.3, 119.6, 116.5, 112.1, 68.6, 59.4, 57.3, 56.6, 44.2, 43.8, 32.1, 27.0, 25.5, 9.9. MS (FAB) *m/z* 432 $[M+H]^+$. HRMS (FAB) calc. for $C_{22}H_{33}N_5O_2S$ $[M + H]^+$ 432.2433, found 432.2441.

1-(3-Methoxy-4-(3-(piperidin-1-yl)propoxy)phenyl)-3-(3-(5-methyl-1*H*-imidazol-1-yl)propyl) thiourea (186). From compound **107**, procedure **5**. yield 30%, white solid, mp 145-146 ^{o}C. ^{1}H NMR (300 MHz, CD_3OD) δ 7.52 (s, 1H), 6.88 (d, J = 2.73, 1H), 6.86 (d, J = 8.79 Hz, 1H), 6.68 (dd, J = 8.58, 2.37 Hz, 1H), 6.58 (s, 1H), 4.01 (t, J = 5.88 Hz, 2H), 3.89 (t, J = 6.96 Hz, 2H), 3.74 (s, 3H), 3.50 (m, 2H), 2.99-2.96 (m, 6H), 2.13 (d, J = 0.9 Hz, 3H), 2.09 - 2.06 (m, 2H), 1.95 (quintet, J = 6.93 Hz, 2H), 1.73 - 1.69 (m, 4H), 1.54 (m, 2H). ^{13}C NMR (125 MHz, CD_3OD) δ 183.5, 152.0, 148.5, 138.8, 133.9, 129.8, 127.2, 119.6, 116.1, 112.0, 69.3, 57.6, 57.3, 55.7, 44.2, 43.7, 32.5, 26.6, 25.7, 24.2, 9.9. MS (FAB) *m/z* 446 $[M+H]^+$. HRMS (FAB) calc. for $C_{23}H_{35}N_5O_2S$ $[M + H]^+$ 446.2591, found 446.2600.

1-(3-Methoxy-4-(4-(piperidin-1-yl)butoxy)phenyl)-3-(3-(5-methyl-1*H*-imidazol-1-yl)propyl)thiourea (187). From compound **108**, procedure **5**. yield 54%, white solid, mp 86-87 ^{o}C. ^{1}H NMR (300 MHz, CD_3OD) δ 7.73 (s, 1H), 6.99 (d, J = 2.37 Hz, 1H), 6.93 (d, J = 8.61 Hz, 1H), 6.78 (dd, J = 8.43, 2.37 Hz, 1H), 6.72 (s, 1H), 4.05-3.98 (m, 4H), 3.81 (s, 3H), 3.59 (t, J = 6.6 Hz, 2H), 3.18-3.09 (m, 6H), 2.23 (d, J = 1.11 Hz, 3H), 2.05 (quintet, J = 6.96 Hz, 2H), 1.97-1.90 (m, 2H), 1.85 (quintet, J = 5.67 Hz, 6H), 1.64 (m, 2H). ^{13}C NMR (125 MHz, $CDCl_3$) δ 181.3, 149.1, 145.8, 136.3, 131.7, 127.6, 124.2, 116.9, 113.1, 109.5, 68.3, 56.8, 55.7, 52.9, 42.5, 41.2, 29.6, 26.2, 22.7, 22.0, 20.9, 9.2. MS (FAB) m/z 460 $[M+H]^+$. HRMS (FAB) calc. for $C_{24}H_{37}N_5O_2S$ $[M+H]^+$ 460.2741, found 460.2754.

1-(3-Methoxy-4-(2-morpholinoethoxy)phenyl)-3-(3-(5-methyl-1*H*-imidazol-1-yl)propyl)thiourea (188). From compound **109**, procedure **5**. yield 53%, white solid, mp 104-105 ^{o}C. ^{1}H NMR (300 MHz, CD_3OD) δ 7.59 (s, 1H), 6.98 (d, J = 8.61 Hz, 1H), 6.92 (d, J = 2.19 Hz, 1H), 6.76 (dd, J = 8.43, 2.4 Hz, 1H), 6.66 (s, 1H), 4.16 (t, J = 5.49 Hz, 2H), 3.99 (t, J = 7.14

Hz, 2H), 3.80 (s, 3H), 3.71 (t, *J* = 4.56 Hz, 4H), 3.61 (t, *J* = 6.60 Hz, 2H), 2.82 (t, *J* = 5.49 Hz, 2H), 2.63 (t, *J* = 4.59 Hz, 4H), 2.22 (d, *J* = 0.9 Hz, 3H), 2.07 (quintet, *J* = 7.35 Hz, 2H). ^{13}C NMR (200 MHz, CD_3OD) δ 183.4, 152.4, 148.9, 138.8, 133.6, 129.7, 127.4, 119.6, 116.5, 112.1, 69.2, 68.5, 59.5, 57.3, 56.0, 44.2, 43.8, 32.2, 9.9. MS (FAB) *m/z*: 434 $[M+H]^+$. HRMS (FAB) calc. for $C_{21}H_{31}N_5O_3S$ $[M + H]^+$ 434.2226, found 434.2231.

1-(3-Methoxy-4-(3-morpholinopropoxy)phenyl)-3-(3-(5-methyl-1*H*-imidazol-1-yl)propyl)thiourea (189). From compound **110**, procedure **5**. yield 18%, white solid, mp 84-85 ^{o}C. ^{1}H NMR (300 MHz, CD_3OD) δ 7.59 (s, 1H), 6.95 (d, *J* = 8.61 Hz, 1H), 6.91 (d, *J* = 2.37 Hz, 1H), 6.75 (dd, *J* = 8.61, 2.37 Hz, 1H), 6.67 (s, 1H), 4.05 (t, *J* = 6.03 Hz, 2H), 3.98 (t, *J* = 7.14 Hz, 2H), 3.81 (s, 3H), 3.69 (t, *J* = 4.77 Hz, 4H), 3.60 (t, *J* = 6.75 Hz, 2H), 2.56 (t, *J* = 7.32 Hz, 2H), 2.51 (br, 4H), 2.22 (d, *J* = 0.93 Hz, 3H), 2.03 (m, 4H). ^{13}C NMR (125 MHz, CD_3OD) δ 183.2, 151.9, 148.9, 138.5, 132.9, 129.4, 127.3, 119.6, 115.6, 111.9, 69.3, 68.3, 57.3, 57.2, 55.4, 44.0, 43.6, 32.0, 27.8, 9.9. MS (FAB) *m/z* 448 $[M+H]^+$. MS (HR-FAB-MS) *m/z* $[M + H]^+$ calc. for $C_{22}H_{33}N_5O_3S$ 448.2377, found 448.2372

1-(3-Methoxy-4-(4-morpholinobutoxy)phenyl)-3-(3-(5-methyl-1*H*-imidazol-1-yl)propyl)thiourea (190). From compound **111**, procedure **5**. yield 41%, white solid (75 mg, 41%), mp 83-84 ^{o}C. ^{1}H NMR (300 MHz, CD_3OD) δ 7.59 (d, *J* = 1.11 Hz, 1H), 6.94 (d, *J* = 8.58 Hz, 1H), 6.90 (d, *J* = 2.4 Hz, 1H), 6.75 (dd, *J* = 8.43, 2.37 Hz, 1H), 6.66 (s, 1H), 4.02 (t, *J* = 5.88 Hz, 2H), 3.97 (t, *J* = 7.32 Hz, 2H), 3.81 (s, 3H), 3.68 (t, *J* = 4.74 Hz, 4H), 3.59 (t, *J* = 6.75 Hz, 2H), 2.49 - 2.41 (m, 4H), 2.22 (d, *J* = 0.93 Hz, 3H), 2.03 (quintet, *J* = 6.96 Hz, 2H), 1.83 - 1.67 (m, 4H). ^{13}C NMR (75 MHz, CD_3OD) δ 183.2, 152.1, 149.3, 138.7, 132.9, 129.7, 127.3, 119.7,

115.7, 112.1, 70.9, 68.4, 60.5, 57.3, 55.5, 44.2, 43.8, 32.2, 29.1, 24.6, 9.9. MS (FAB) *m/z* 462 $[M+H]^+$. HRMS (FAB) calc. for $C_{23}H_{35}N_5O_3S$ $[M+H]^+$ 462.2533, found 462.2547.

1-(3-Methoxy-4-(2-(piperazin-1-yl)ethoxy)phenyl)-3-(3-(5-methyl-1*H*-imidazol-1-yl)propyl)thiourea (191). From compound **152**, procedure **7**. yield 70%, white solid, mp 81-82 ^oC. ^1H NMR (300 MHz, $CDCl_3$) δ 7.72 (br, 1H), 7.40 (s, 1H), 6.91 (d, J = 8.97 Hz, 1H), 6.75 - 6.72 (m, 3H), 6.04 (br, 1H), 4.17 (t, J = 6.06 Hz, 2H), 3.92 (t, J = 6.96 Hz, 2H), 3.83 (s, 3H), 3.69 (q, J = 6.24 Hz, 2H), 2.95 (t, J = 4.77 Hz, 4H), 2.87 (t, J = 6.06 Hz, 2H), 2.59 (br, 4H), 2.18 (d, J = 0.93 Hz, 3H), 2.10 (quintet, J = 6.96 Hz, 2H). ^{13}C NMR (125 MHz, CD_3OD) δ 183.4, 152.4, 149.0, 138.8, 133.5, 129.7, 127.4, 119.7, 116.5, 112.2, 69.2, 59.6, 57.3, 55.9, 46.8, 44.2, 43.8, 32.2, 9.9. MS (FAB) *m/z* 433 $[M+H]^+$. HRMS (FAB) calc. for $C_{21}H_{32}N_6O_2S$ $[M + H]^+$ 433.2386, found 433.2386.

1-(3-Methoxy-4-(3-(piperazin-1-yl)propoxy)phenyl)-3-(3-(5-methyl-1*H*-imidazol-1-yl)propyl) thiourea (192). From compound **153**, procedure **7**. yield 28%, white solid, mp 73-74 ^oC. ^1H NMR (300 MHz, CD_3OD) δ 7.61 (s, 1H), 6.95 (d, J = 9.51 Hz, 1H), 6.93 (s, 1H), 6.76 (d, J = 8.79 Hz, 1H), 6.68 (s, 1H), 4.06 (t, J = 6.06 Hz, 2H), 3.98 (t, J = 7.5 Hz, 2H), 3.81 (s, 3H), 3.60 (m, 2H), 3.08 (t, J = 5.31 Hz, 4H), 2.63 (br, 6H), 2.23 (s, 3H), 2.06-1.99 (m, 4H). ^{13}C NMR (150 MHz, CD_3OD) δ 183.5, 152.1, 149.1, 138.7, 133.1 129.8, 127.2, 119.7, 115.9, 112.2, 69.3, 57.3, 56.8, 52.7, 45.9, 44.2, 43.7, 32.1, 28.2, 9.9. MS (FAB) *m/z* 447 $[M+H]^+$. HRMS (FAB) calc. for $C_{22}H_{34}N_6O_2S$ $[M+H]^+$ 447.2537,found 447.2524.

1-(3-Methoxy-4-(4-(piperazin-1-yl)butoxy)phenyl)-3-(3-(5-methyl-1*H*-imidazol-1-yl)propyl)thiourea (193). From compound **154**, procedure **7**. yield 54%, white solid, mp 80-81

°C. ^{1}H NMR (300 MHz, CD_3OD) δ 7.62 (s, 1H), 6.94 (d, J = 8.04 Hz, 1H), 6.92 (s, 1H), 6.75 (d, J = 8.61 Hz, 1H), 6.68 (s, 1H), 4.04-3.96 (m, 4H), 3.81 (s, 3H), 3.59 (t, J = 6.39 Hz, 2H), 3.09 (br, 4H), 2.64 (br, 4H), 2.51 (t, J = 7.14 Hz, 2H), 2.22 (s, 3H), 2.04 (quintet, J = 6.78 Hz, 2H), 1.81 - 1.71 (m, 4H). ^{13}C NMR (200 MHz, CD_3OD) δ 183.4, 152.0, 149.1, 138.7, 133.1, 129.8, 127.1, 119.6, 115.7, 112.1, 70.9, 59.7, 57.3, 52.4, 45.6, 44.2, 43.7, 32.1, 28.8, 24.7, 9.9. MS(FAB) *m/z* 461 $[M+H]^+$. HRMS (FAB) calc. for $C_{23}H_{36}N_6O_2S$ $[M+H]^+$ 461.2693, found 461.2695.

1-(3-Methoxy-4-(2-(4-methylpiperazin-1-yl)ethoxy)phenyl)-3-(3-(5-methyl-1*H*-imidazol-1-yl)propyl)thiourea (194). From compound **112**, procedure **5**. yield 60%, white solid, mp 94-95 °C. ^{1}H NMR (300 MHz, CD_3OD) δ 7.59 (d, J = 1.11 Hz, 1H), 6.97 (d, J = 8.61 Hz, 1H), 6.91 (d, J = 2.37 Hz, 1H), 6.76 (dd, J = 8.4, 2.37 Hz, 1H), 6.66 (s, 1H), 4.15 (t, J = 5.49 Hz, 2H), 3.99 (t, J = 7.32 Hz, 2H), 3.80 (s, 3H), 3.59 (t, J = 6.78 Hz, 2H), 2.83 (t, J = 5.31 Hz, 2H), 2.50 (br, 8H), 2.28 (s, 3H), 2.22 (d, J = 0.93 Hz, 3H), 2.05 (quintet, J = 6.78 Hz, 2H). ^{13}C NMR (200 MHz, CD_3OD) δ 183.4, 153.3, 149.0, 138.8, 133.7, 129.7, 127.4, 119.7, 116.5, 112.2, 70.5, 59.2, 57.3, 56.4, 54.9, 46.8, 44.2, 43.8, 32.2, 9.9. MS(FAB) *m/z* 447 $[M+H]^+$. HRMS (FAB) calc. for $C_{22}H_{34}N_6O_2S$ $[M + H]^+$ 447.2542, found 447.2539.

1-(3-Methoxy-4-(3-(4-methylpiperazin-1-yl)phenyl)-3-(3-(5-methyl-1*H*-imidazol-1-yl)propyl)thiourea (195). From compound **113**, procedure **5**. yield 19%, white solid, mp 65-66 °C. ^{1}H NMR (300 MHz, CD_3OD) δ 7.59 (d, J = 1.08 Hz, 1H), 6.95 (d, J = 8.61 Hz, 1H), 6.90 (d, J = 2.19 Hz, 1H), 6.75 (dd, J = 8.4, 2.37 Hz, 1H), 6.67 (s, 1H), 4.02 (t, J = 6.24 Hz, 2H), 3.98 (t, J = 7.14 Hz, 2H), 3.81 (s, 3H), 3.60 (t, J = 7.14 Hz, 2H), 2.58 (br, 10H), 2.29 (s, 3H), 2.22 (d, J = 1.11 Hz, 3H), 2.01 (m, 4H). ^{13}C NMR (125 MHz, CD_3OD) δ 183.3, 153.2, 149.2, 138.7, 133.1, 129.6, 127.3, 119.7, 115.9, 112.2, 69.4, 57.3, 56.9, 56.4, 54.4, 46.8, 44.1, 43.8, 32.1, 28.3, 9.9.

MS(FAB) *m/z* 461 $[M+H]^+$. HRMS (FAB) calc. for $C_{23}H_{36}N_6O_2S$ $[M+H]^+$ 461.2693, found 461.2695.

1-(3-Methoxy-4-(4-(4-methylpiperazin-1-yl)butoxy)phenyl)-3-(3-(5-methyl-1*H*-imidazol-1-yl)propyl)thiourea (196). From compound **114**, procedure **5**. yield 64%, white solid, mp 83-84 ^oC. ^1H NMR (300 MHz, CD_3OD) δ 8.27 (s, 1H), 6.98 - 6.91 (m, 3H), 6.79 (m, J = 8.43 Hz, 1H), 4.10 (t, J = 7.14 Hz, 2H), 4.03 (m, 2H), 3.81 (s, 3H), 3.61 (m, 2H), 2.98 (m, 8H), 2.73 (m, 2H), 2.63 (s, 3H), 2.29 (s, 3H), 2.10 (quintet, J = 6.78 Hz, 2H), 1.81 (m, 4H). ^{13}C NMR (150 MHz, CD_3OD) δ 183.5, 151.8, 148.7, 137.9, 133.9, 131.4, 123.3, 119.4, 115.7, 112.1, 70.8, 58.9, 57.4, 54.9, 52.6, 45.3, 43.2, 43.3, 31.5, 28.6, 24.3, 9.9. MS(FAB) *m/z* 475 $[M+H]^+$. HRMS (FAB) calc. for $C_{24}H_{38}N_6O_2S$ $[M+H]^+$ 475.2850, found 475.2862.

1-(3-Methoxy-4-(2-(piperidin-4-yl)ethoxy)phenyl)-3-(3-(5-methyl-1*H*-imidazol-1-yl)propyl)thiourea (197). From compound **155**, procedure **7**. yield 82%, white solid, the compound was decomposed at 199 ^oC. ^1H NMR (300 MHz, CD_3OD) δ 7.50 (d, J = 1.11 Hz, 1H), 6.86 (d, J = 8.43 Hz, 1H), 6.81 (d, J = 2.37 Hz, 1H), 6.67 (dd, J = 8.43, 2.37 Hz, 1H), 6.57 (s, 1H), 3.97 (t, J = 6.06 Hz, 2H), 3.90 (t, J = 7.14 Hz, 2H), 3.72 (s, 3H), 3.50 (t, J = 7.14 Hz, 2H), 3.02-2.97 (m, 2H), 2.60 (td, J = 10.44, 2.01 Hz, 2H), 2.13 (d, J = 1.11 Hz, 3H), 1.96 (quintet, J = 6.78 Hz, 4H), 1.79-1.74 (m, 3H), 1.69 - 1.64 (m, 2H). ^{13}C NMR (200 MHz, CD_3OD) δ 183.5, 152.2, 149.1, 138.8, 133.2, 129.7, 127.4, 119.7, 115.9, 112.1, 68.7, 57.3, 46.5, 44.2, 43.8, 37.3, 32.1, 31.7, 31.6, 9.9. MS(FAB) *m/z* 432 $[M+H]^+$. HRMS (FAB) calc. for $C_{22}H_{33}N_5O_2S$ $[M + H]^+$ 432.2428, found 432.243

1-(3-Methoxy-4-(3-(piperidin-4-yl)propoxy)phenyl)-3-(3-(5-methyl-1*H*-imidazol-1-yl)propyl)thiourea (198). From compound **156**, procedure **7**. yield 64%, white solid, mp 153-154 ^{o}C. ^{1}H NMR (300 MHz, CD_3OD) δ 7.59 (s, 1H), 6.95 (d, J = 4.23 Hz, 1H), 6.92 (d, J = 1.83 Hz, 1H), 6.77 (dd, J = 8.58, 2.37 Hz, 1H), 6.67 (s, 1H), 4.02 (q, J = 6.03 Hz, 4H), 3.81 (s, 3H), 3.59 (t, J = 7.14 Hz, 2H), 3.38 (t, J = 7.14 Hz, 2H), 2.97-2.90 (m, 2H), 2.22 (d, J = 1.08 Hz, 3H), 2.06-1.95 (m, 4H), 1.89-1.80 (m, 2H), 1.65 (br, 1H), 1.53 - 1.48 (m, 2H), 1.38-1.28 (m, 2H). ^{13}C NMR (150 MHz, CD_3OD) δ 183.4, 152.1, 149.2, 138.8, 133.2, 129.8, 127.2, 119.8, 115.7, 112.2, 71.2, 57.3, 46.1, 44.2, 43.8, 35.5, 34.5, 32.1, 30.9, 28.0, 9.9. MS(FAB) *m/z* 446 $[M+H]^+$. HRMS (FAB) calc. for $C_{23}H_{35}N_5O_2S$ $[M + H]^+$ 446.2584, found 446.2590.

1-(3-Methoxy-4-(4-(piperidin-4-yl)butoxy)phenyl)-3-(3-(5-methyl-1*H*-imidazol-1-yl)propyl)thiourea (199). From compound **147**, procedure **7**. yield 64%, white solid, mp 95-96 ^{o}C. ^{1}H NMR (300 MHz, CD_3OD) δ 7.59 (d, J = 1.11 Hz, 1H), 6.95 (d, J = 8.61 Hz, 1H), 6.90 (d, J = 2.40 Hz, 1H), 6.76 (dd, J = 8.61, 2.37 Hz, 1H), 6.66 (s, 1H), 4.01 (q, J = 6.39 Hz, 4H), 3.81 (s, 3H), 3.62 (t, J = 6.96, 2H), 3.10 - 3.05 (m, 2H), 2.67 - 2.59 (m, 2H), 2.22 (d, J = 0.93 Hz, 3H), 2.08 (quintet, J = 6.78 Hz, 2H), 1.77-1.74 (m, 4H), 1.51-1.46 (m, 3H), 1.35-1.30 (m, 2H), 1.23-1.14 (m, 2H). ^{13}C NMR (200 MHz, CD_3OD) δ 183.4, 152.1, 149.3, 138.8, 133.1, 129.7, 127.3, 119.7, 115.7, 112.2, 71.1, 57.4, 47.2, 44.2, 43.8, 38.3, 37.0, 33.2, 32.2, 31.2, 24.8, 9.9. MS(FAB) *m/z* 460 $[M+H]^+$. HRMS (FAB) calc. for $C_{24}H_{37}N_5O_2S$ $[M + H]^+$ 460.2741, found 460.2746.

1-(3-Methoxy-4-(2-(1-methylpiperidin-4-yl)ethoxy)phenyl)-3-(3-(5-methyl-1*H*-imidazol-1-yl)propyl)thiourea (200). From compound **115**, procedure **5**. yield 34%, white solid, mp 111-112 ^{o}C. ^{1}H NMR (300 MHz, CD_3OD) δ 7.50 (d, J = 1.11 Hz, 1H), 6.86 (d, J = 8.61 Hz, 1H), 6.80 (d, J = 2.40 Hz, 1H), 6.67 (dd, J = 8.61, 2.40 Hz, 1H), 6.57 (br, 1H), 3.96 (t, J = 6.39 Hz, 2H),

3.90 (t, J = 7.32 Hz, 2H), 3.71 (s, 3H), 3.52 (q, J = 7.14 Hz, 2H), 2.79 - 2.75 (m, 2H), 2.15 (s, 3H), 2.13 (d, J = 0.93 Hz, 3H), 1.96 - 1.88 (m, 4H), 1.71-1.60 (m, 4H), 1.48 (br, 1H), 1.26 - 1.18 (m, 2H). ^{13}C NMR (125 MHz, CD_3OD) δ 183.3, 152.2, 149.3, 138.8, 133.1, 129.7, 127.4, 119.8, 115.9, 112.2, 68.9, 57.3, 46.9, 44.2, 43.8, 37.5, 33.8, 33.5, 32.2, 9.9. MS(FAB) *m/z* 446 $[M+H]^+$. HRMS (FAB) calc. for $C_{23}H_{35}N_5O_2S$ $[M + H]^+$ 446.2590, found 446.2590.

1-(3-Methoxy-4-(3-(1-methylpiperidin-4-yl)propoxy)phenyl)-3-(3-(5-methyl-1*H*-imidazol-1-yl)propyl)thiourea (201). From compound **116**, procedure **5**. yield 40%, light yellow solid, mp 168-169 ^{o}C. ^{1}H NMR (300 MHz, CD_3OD) δ 7.65 (s, 1H), 6.85-6.82 (m, 2H), 6.67 - 6.64 (m, 2H), 3.92 (t, J = 6.03 Hz, 4H), 3.72 (s, 3H), 3.50 (t, J = 6.96 Hz, 2H), 3.36 (br, 1H), 3.32 (br, 1H), 2.86 (t, J = 11.34 Hz, 2H), 2.71 (s, 3H), 2.14 (d, J = 0.93 Hz, 3H), 1.97-1.89 (m, 4H), 1.71 (m, 2H), 1.52 - 1.31 (m, 5H). ^{13}C NMR (75 MHz, CD_3OD) δ 183.4, 152.1, 149.2, 139.2, 133.2, 130.1, 126.6, 119.7, 115.7, 112.2, 71.2, 57.3, 56.5, 44.8, 44.4, 43.7, 34.9, 34.0, 32.0, 31.6, 28.2, 9.9. MS(FAB) *m/z* 460 $[M+H]^+$. HRMS (FAB) calc. for $C_{24}H_{37}N_5O_2S$ $[M + H]^+$ 460.2746, found 460.2746.

1-(3-Methoxy-4-(4-(1-methylpiperidin-4-yl)butoxy)phenyl)-3-(3-(5-methyl-1*H*-imidazol-1-yl)propyl)thiourea (202). Prepared from compound **199** by following the experiment procedure used for compound **22** to afford the desired product as a white solid (36 mg, 38%), mp 113-114 ^{o}C. ^{1}H NMR (300 MHz, CD_3OD) δ 7.49 (d, J = 1.11 Hz, 1H), 6.84-6.80 (m, 2H), 6.67 (dd, J = 8.40, 2.37 Hz, 1H), 6.56 (s, 1H), 3.91 - 3.85 (m, 4H), 3.71 (s, 3H), 3.52 (quintet, J = 6.96 Hz, 2H), 2.76 (br, 1H), 2.72 (br, 1H), 2.13 (s, 3H), 2.12 (d, J = 0.90 Hz, 3H), 1.98 - 1.88 (m, 4H), 1.71 - 1.62 (m, 5H), 1.36 - 1.33 (m, 2H), 1.23 - 1.10 (m, 4H). ^{13}C NMR (200 MHz, CD_3OD) δ 183.4, 152.1, 149.4, 138.8, 133.1, 129.7, 127.3, 119.7, 115.7, 112.2, 71.1, 57.4, 57.2, 46.3, 44.2, 43.8,

37.7, 36.2, 33.0, 32.2, 31.2, 25.0, 9.9. MS(FAB) *m/z* 474 $[M+H]^+$. HRMS (FAB) calc. for $C_{25}H_{39}N_5O_2S$ $[M + H]^+$ 474.2902, found 474.2903.

1-(4-(4-Aminophenethoxy)-3-methoxyphenyl)-3-(3-(5-methyl-1*H*-imidazol-1-yl)propyl)thiourea (203). From compound **157**, procedure **7**. yield 68%, white solid, mp 74-75 ^oC. ^1H NMR (300 MHz, CD_3OD) δ 7.58 (d, J = 1.11 Hz, 1H), 7.05-7.02 (m, 2H), 6.92 (d, J = 8.40 Hz, 1H), 6.89 (d, J = 2.37 Hz, 1H), 6.74 (dd, J = 8.43, 2.40 Hz, 1H), 6.68-6.65 (m, 3H), 4.10 (t, J = 7.14 Hz, 2H), 3.98 (t, J = 7.32 Hz, 2H), 3.80 (s, 3H), 3.60 (q, J = 6.96 Hz, 2H), 2.95 (t, J = 7.14 Hz, 2H), 2.21 (d, J = 1.08 Hz, 3H), 2.06 (quintet, J = 7.14 Hz, 2H). ^{13}C (150 MHz, $CDCl_3$) δ 181.7, 150.4, 148.0, 145.0, 136.5, 129.8, 128.7, 127.4, 126.9, 126.8, 118.5, 115.2, 113.4, 110.3, 70.4, 56.2, 42.3, 42.2, 34.8, 30.3, 9.2. MS(ESI) *m/z* 440 $[M+H]^+$. HRMS (FAB) calc. for $C_{23}H_{29}N_5O_2S$ $[M + H]^+$ 440.2120, found 440.2118.

1-(4-(3-(4-Aminophenyl)propoxy)-3-methoxyphenyl)-3-(3-(5-methyl-1*H*-imidazol-1-yl)propyl)thiourea (204). From compound **158**, procedure **7**. yield 62%, white solid, mp 58-59 ^oC. ^1H NMR (300 MHz, $CDCl_3$) δ 7.52 (s, 1H), 7.37 (s, 1H), 7.00 (d, J = 8.43 Hz, 2H), 6.83 (d, J = 8.97 Hz, 1H), 6.73-6.68 (m, 3H), 6.63 (d, J = 8.22 Hz, 2H), 5.90 (br, 1H), 4.02 (t, J = 6.57 Hz, 2H), 3.90 (t, J = 7.14 Hz, 2H), 3.84 (s, 3H), 3.69 (q, J = 6.42 Hz, 2H), 2.72 (t, J = 7.14 Hz, 2H), 2.21 (d, J = 0.93 Hz, 3H), 2.17 - 1.99 (m, 4H). ^{13}C NMR (75 MHz, CD_3OD) δ 183.2, 152.1, 149.3, 147.0, 138.7, 133.4, 132.8, 130.1, 129.7, 119.8, 117.7, 115.7, 115.7, 112.1, 70.2, 57.4, 44.2, 43.8, 33.1, 32.9, 32.2, 9.9. MS(FAB) *m/z* 454 $[M+H]^+$. HRMS (FAB) calc. for $C_{24}H_{31}N_5O_2S$ $[M + H]^+$ 454.2277, found 454.2274.

1-(4-(4-(4-Aminophenyl)butoxy)-3-methoxyphenyl)-3-(3-(5-methyl-1*H*-imidazol-1-yl)propyl)thiourea (205). From compound **159**, procedure **7**. yield 62%, white solid, mp 59-60 ^{o}C. ^{1}H NMR (300 MHz, $CDCl_3$) δ 7.57 (s, 1H), 7.37 (s, 1H), 6.99 (d, J = 8.40 Hz, 2H), 6.85 (d, J = 8.43 Hz, 1H), 6.72 - 6.67 (m, 3H), 6.64 - 6.59 (m, 2H), 5.92 (br, NH), 4.03 (t, J = 6.42 Hz, 2H), 3.90 (t, J = 7.14 Hz, 2H), 3.82 (s, 3H), 3.69 (q, J = 6.24 Hz, 2H), 2.60 (t, J = 7.53 Hz, 2H), 2.17 (d, J = 0.93 Hz, 3H), 2.08 (quintet, J = 6.93 Hz, 2H), 1.94 - 1.69 (m, 4H). ^{13}C NMR (150 MHz, CD_3OD) δ 183.2, 152.1, 149.4, 146.9, 138.7, 134.2, 132.8, 130.8, 129.7, 127.3, 119.8, 117.7, 115.8, 112.2, 71.2, 57.4, 44.2, 43.8, 36.5, 32.1, 30.6, 30.1, 9.9. MS(FAB) *m/z* 468 $[M+H]^+$. HRMS (FAB) calc. for $C_{25}H_{33}N_5O_2S$ $[M + H]^+$ 468.2433, found 468.2425.

1-(3-Methoxy-4-(2-(pyridin-4-yl)ethoxy)phenyl)-3-(3-(5-methyl-1*H*-imidazol-1-yl)propyl)thiourea (206). From compound **117**, procedure **5**. yield 63%, white solid, mp 114-115 ^{o}C. ^{1}H NMR (300 MHz, CD_3OD) δ 8.42 (dd, J = 4.38, 1.47 Hz, 2H), 7.61 (d, J = 1.11 Hz, 1H), 7.43 (dd, J = 4.59, 1.65 Hz, 2H), 6.94 (d, J = 8.61 Hz, 1H), 6.90 (d, J = 2.19 Hz, 1H), 6.73 (dd, J = 8.43, 2.37 Hz, 1H), 6.67 (s, 1H), 4.26 (t, J = 6.21 Hz, 2H), 3.97 (t, J = 7.14 Hz, 2H), 3.78 (s, 3H), 3.58 (t, J = 5.85 Hz, 2H), 3.13 (t, J = 6.21 Hz, 2H), 2.21 (d, J = 1.11 Hz, 3H), 2.02 (quintet, J = 6.96 Hz, 2H). ^{13}C NMR (200 MHz, $CDCl_3$) δ 181.2, 150.0, 148.9, 147.9, 146.7, 136.2, 130.1, 127.1, 125.8, 124.5, 117.7, 113.8, 110.0, 68.5, 55.8, 42.1, 41.7, 34.7, 30.0, 9.2. MS(FAB) *m/z* 426 $[M+H]^+$. HRMS (FAB) calc. for $C_{22}H_{27}N_5O_2S$ $[M+H]^+$ 426.1958, found 426.1962.

1-(3-Methoxy-4-(4-(pyridin-4-yl)propoxy)phenyl)-3-(3-(5-methyl-1*H*-imidazol-1-yl)propyl)thiourea (207). From compound **118**, procedure **5**. yield 26%, white solid, mp 81-82 ^{o}C. ^{1}H NMR (600 MHz, CD_3OD) δ 8.39 (dd, J = 4.56, 1.32 Hz, 2H), 7.59 (s, 1H), 7.32 (d, J =

6.42 Hz, 2H), 6.93 (br, 2H), 6.75 (dd, *J* = 8.28, 2.28 Hz, 1H), 6.66 (s, 1H), 4.00 (t, *J* = 6.42 Hz, 2H), 3.97 (t, *J* = 7.32 Hz, 2H), 3.83 (s, 3H), 3.60 (t, *J* = 6.42 Hz, 2H), 2.88 (t, *J* = 7.32 Hz, 2H), 2.22 (s, 3H), 2.15-2.10 (m, 2H), 2.03 (quintet, *J* = 7.32 Hz, 2H). ^{13}C NMR (125 MHz, CD_3OD) δ 183.4, 154.6, 152.2, 150.7, 149.0, 138.8, 133.4, 129.7, 127.4, 126.6, 119.7, 116.0, 112.1, 70.1, 57.3, 44.2, 43.8, 33.3, 32.2, 31.7, 9.9. MS(FAB) *m/z* 440 $[M+H]^+$. HRMS (FAB) calc. for $C_{23}H_{29}N_5O_2S$ $[M+H]^+$ 440.2115, found 440.2121.

1-(3-(1*H*-Imidazol-1-yl)propyl)-3-(3-methoxy-4-(4-(pyridin-4-yl)butoxy)phenyl)thiourea (208). From compound **119**, procedure **5**, yield 45%, white solid, mp 58-59 ^{o}C. ^{1}H NMR (500 MHz, $CDCl_3$) δ 8.43 (d, *J* = 6.06 Hz, 2H), 7.51 (s, 1H), 7.36 (s, 1H), 7.12 (d, *J* = 5.85 Hz, 2H), 6.79 (d, *J* = 8.97 Hz, 1H), 6.73 (s, 1H), 6.71 - 6.68 (m, 2H), 6.04 (s, 1H), 4.01 (m, 2H), 3.89 (t, *J* = 7.14 Hz, 2H), 3.84 (s, 3H), 3.67 (q, *J* = 7.53 Hz, 2H), 2.70 (m, 2H), 2.17 (d, *J* = 0.9 Hz, 3H), 2.06 (quintet, *J* = 7.14 Hz, 2H), 1.88-1.86 (m, 4H). ^{13}C NMR (75 MHz, CD_3OD) δ 183.3, 155.2, 152.1, 150.6, 149.3, 138.8, 133.0, 129.7, 127.3, 126.5, 119.8, 115.7, 112.2, 70.9, 57.3, 44.2, 43.8, 36.5, 32.2, 30.6, 28.8, 9.9. MS(ESI) *m/z* 454 $[M+H]^+$. HRMS (FAB) calc. for $C_{24}H_{31}N_5O_2S$ $[M+H]^+$ 454.2276, found 454.2273.

1-(3-Methoxy-4-(4-(pyridin-3-yl)butoxy)phenyl)-3-(3-(5-methyl-1*H*-imidazol-1-yl)propyl)thiourea (209). From compound **122**, procedure **5**. yield 52%, white solid, mp 70-71 ^{o}C. ^{1}H NMR (300 MHz, $CDCl_3$) δ 8.42 (d, *J* = 1.44 Hz, 1H), 8.40 (d, *J* = 1.65 Hz, 1H), 7.62 (s, 1H), 7.52 (d, *J* = 7.68 Hz, 1H), 7.41 (s, 1H), 7.23 (dd, *J* = 7.68, 4.95 Hz, 1H), 6.84 (d, *J* = 8.97 Hz, 1H), 6.73-6.71 (m, 3H), 6.13 (br, 1H), 4.06 (t, *J* = 5.57 Hz, 2H), 3.92 (t, *J* = 7.14 Hz, 2H), 3.82 (s, 3H), 3.70 (q, *J* = 6.39 Hz, 2H), 2.72 (t, *J* = 7.14 Hz, 2H), 2.17 (s, 3H), 2.10 (quintet, *J* = 6.93 Hz, 2H), 1.88-1.81 (m, 4H). ^{13}C NMR (200 MHz, $CDCl_3$) δ 181.2, 149.8, 148.9, 147.3,

146.5, 137.6, 136.4, 136.1, 129.4, 127.2, 125.6, 123.4, 117.9, 113.1, 109.8, 68.7, 55.8, 42.2, 41.7, 32.3, 29.9, 28.2, 27.2, 9.2. MS (FAB) *m/z* 454 $[M+H]^+$. HRMS (FAB) calc. for $C_{24}H_{31}N_5O_2S$ [M + H]$^+$ 454.2277, found 454.2277.

1-(4-(2-(2-Aminopyridin-4-yl)ethoxy)-3-methoxyphenyl)-3-(3-(5-methyl-1*H*-imidazol-1-yl)propyl) thiourea (210). From compound **160**, procedure **7**. yield 41%, white solid, mp 60-61 ^oC. ^1H NMR (300 MHz, CD_3OD) δ 7.77 (d, J = 5.49 Hz, 1H), 7.59 (d, J = 2.40 Hz, 1H), 6.94 (d, J = 8.43 Hz, 1H), 6.90 (d, J = 2.40 Hz, 1H), 6.73 (dd, J = 8.40, 2.37 Hz, 1H), 6.66 (s, 1H), 6.59 (dd, J = 5.52, 1.26 Hz, 1H), 6.54 (s, 1H), 4.20 (t, J = 6.60 Hz, 2H), 3.97 (t, J = 6.96 Hz, 2H), 3.79 (s, 3H), 3.59 (t, J = 6.78 Hz, 2H), 2.96 (t, J = 6.39 Hz, 2H), 2.21 (d, J = 1.11 Hz, 3H), 2.02 (quintet, J = 6.42 Hz, 2H). ^{13}C NMR (150 MHz, CD_3OD) δ 183.9, 161.7, 154.8, 152.4, 149.1, 148.3, 138.8, 133.2, 129.7, 127.3, 119.8, 116.5, 115.9, 111.3, 110.3, 71.0, 57.5, 44.2, 43.8, 36.9, 32.2, 9.9. MS (FAB) *m/z* 441 $[M+H]^+$. HRMS (FAB) calc. for $C_{22}H_{28}N_6O_2S$ $[M+H]^+$ 441.2067, found 441.2080.

1-(4-(3-(2-Aminopyridin-4-yl)propoxy)-3-methoxyphenyl)-3-(3-(5-methyl-1*H*-imidazol-1-yl)propyl) thiourea (211). From compound **161**, procedure **7**. yield 22%, white solid, mp 148-149 ^oC. ^1H NMR (500 MHz, CD_3OD) δ 7.75 (d, J = 5.40 Hz, 1H), 7.58 (s, 1H), 6.93-6.91 (m, 2H), 6.74 (dd, J = 8.40, 2.10 Hz, 1H), 6.66 (s, 1H), 6.50 (d, J = 5.35 Hz, 1H), 6.45 (s, 1H), 4.00 - 3.96 (m, 4H), 3.83 (s, 3H), 3.59 (t, J = 6.35 Hz, 2H), 2.70 (t, J = 7.45 Hz, 2H), 2.22 (s, 3H), 2.09-2.00 (m, 4H). ^{13}C NMR (125 MHz, CD_3OD) δ 183.4, 161.8, 155.3, 152.3, 149.3, 148.4, 138.8, 133.6, 129.7, 127.4, 119.8, 116.2, 115.7, 112.3, 110.7, 70.3, 57.4, 44.2, 43.8, 33.3, 32.2, 31.6, 9.9.

MS (FAB) *m/z* 455 $[M+H]^+$. HRMS (FAB) calc. for $C_{23}H_{30}N_6O_2S$ $[M+H]^+$ 455.2224, found 455.2235.

1-(4-(4-(2-Aminopyridin-4-yl)butoxy)-3-methoxyphenyl)-3-(3-(5-methyl-1*H*-imidazol-1-yl)propyl) thiourea (212). From compound **148**, procedure **7**. yield 84%, white solid, mp 102-103 ^oC. ^1H NMR (300 MHz, CD_3OD) δ 7.75 (d, J = 5.49 Hz, 1H), 7.59 (s, 1H), 6.94-6.90 (m, 2H), 6.74 (dd, J = 8.43, 2.37 Hz, 1H), 6.66 (s, 1H), 6.49 (dd, J = 5.49, 1.47 Hz, 1H), 6.44 (s, 1H), 4.01-3.94 (m, 4H), 3.81 (s, 3H), 3.59 (t, J = 7.14 Hz, 2H), 2.57 (m, 2H), 2.21 (d, J = 0.90 Hz, 3H), 2.05 (quintet, J = 6.96 Hz, 2H), 1.79 (m, 4H). ^{13}C NMR (125 MHz, $CDCl_3$) δ 181.1, 158.5, 153.3, 149.8, 147.2, 146.4, 136.1, 129.5, 127.1, 125.7, 117.8, 114.2, 113.1, 109.9, 108.5, 68.7, 55.7, 42.1, 41.7, 34.5, 30.0, 28.3, 26.1, 9.2. MS (FAB) *m/z* 469 $[M+H]^+$. HRMS (FAB) calc. for $C_{24}H_{32}N_6O_2S$ $[M+H]^+$ 469.2380, found 469.2377.

***N*-(4-(4-(2-Methoxy-4-(3-(3-(5-methyl-1*H*-imidazol-1-yl)propyl)thioureido)phenoxy)butyl)pyridin-2-yl)acetamide (213)**. Prepared from compound **212** (1.0 equiv) by following the experiment procedure used for compound **178** to afford the desired product as a white solid (44%), the compound was decomposed at 211 ^oC. ^1H NMR (300 MHz, $CDCl_3$) δ 8.69 (s, 1H), 8.08 (s, 1H), 8.06 (d, J = 2.94 Hz, 1H), 8.00 (s, 1H), 7.46 (s, 1H), 6.88 (d, J = 5.13 Hz, 1H), 6.84 (d, J = 8.25 Hz, 1H), 6.74-6.71 (m, 3H), 6.04 (s, 1H), 4.03 (t, J = 5.67 Hz, 2H), 3.91 (t, J = 6.96 Hz, 2H), 3.83 (s, 3H), 3.67 (q, J = 6.39 Hz, 2H), 2.71 (t, J = 7.14 Hz, 2H), 2.21 (s, 3H), 2.18 (s, 3H), 2.06 (quintet, J = 6.96 Hz, 2H), 1.87 (m, 4H). ^{13}C NMR (125 MHz, $CDCl_3$) δ 181.8, 168.8, 153.9, 151.5, 150.5, 148.3, 147.4, 136.6, 129.8, 128.3, 127.0, 120.1,

118.7, 113.7, 113.3, 110.2, 68.8, 56.1, 42.4, 42.3, 35.1, 30.4, 28.5, 26.7, 24.8, 9.2. MS (ESI) *m/z* 511 $[M+H]^+$. HRMS (FAB) calc. for $C_{26}H_{34}N_6O_3S$ $[M+H]^+$ 511.2492, found 511.2500.

1-(4-(3-(2,6-Diaminopyridin-4-yl)propoxy)-3-methoxyphenyl)-3-(3-(5-methyl-1*H*-imidazol-1-yl) propyl)thiourea (214). From compound **162**, procedure **7**. yield 11%, white solid, the compound was decomposed at 151 ^oC. ^1H NMR (300 MHz, $CDCl_3$ + 5% CD_3OD) δ 7.42 (s, 1H), 6.84 (d, J = 8.43 Hz, 1H), 6.79 (d, J = 2.37 Hz, 1H), 6.73 (dd, J = 8.22, 2.37 Hz, 1H), 6.70 (s, 1H), 5.77 (s, 2H), 4.00 (t, J = 6.24 Hz, 2H), 3.91 (t, J = 7.32 Hz, 2H), 3.86 (s, 3H), 3.64 (t, J = 7.14 Hz, 2H), 2.59 (t, J = 7.86 Hz, 2H), 2.20 (s, 3H), 2.12-2.03 (m, 4H). ^{13}C NMR (150 MHz, CD_3OD) δ 183.7, 160.6, 156.7, 152.3, 149.4, 138.8, 133.2, 129.7, 127.4, 119.9, 116.1, 112.3, 99.2, 70.4, 57.4, 44.2, 43.8, 33.4, 32.2, 31.6, 9.9. MS (ESI) *m/z* 470 $[M+H]^+$. HRMS (FAB) calc. for $C_{23}H_{31}N_7O_2S$ $[M+H]^+$ 470.2338, found 470.2331.

1-(4-(3-(2,6-Diaminopyridin-4-yl)butoxy)-3-methoxyphenyl)-3-(3-(5-methyl-1*H*-imidazol-1-yl) propyl)thiourea (215). From compound **163**, procedure **7**. yield 31%, white solid, the compound was decomposed at 145 ^oC. ^1H NMR (300 MHz, $CDCl_3$) δ 7.58 (s, 1H), 7.37 (s, 1H), 6.84 (d, J = 8.22 Hz, 1H), 6.73-6.68 (m, 3H), 5.96 (s, 1H), 5.75 (s, 2H), 4.13 (br, 4H), 4.01 (t, J = 6.24 Hz, 2H), 3.89 (t, J = 7.14 Hz, 2H), 3.84 (s, 3H), 3.66 (q, J = 7.71 Hz, 2H), 2.46 (t, J = 7.32 Hz, 2H), 2.17 (d, J = 0.93 Hz, 2H), 2.05 (quintet, J = 7.14 Hz, 2H), 1.88-1.72 (m, 4H). ^{13}C NMR (150 MHz, CD_3OD) δ 183.4, 160.5, 157.3, 152.2, 149.3, 138.8, 133.2, 129.7, 127.4, 119.8, 115.9, 112.3, 99.3, 71.1, 57.4, 44.2, 43.8, 36.8, 32.2, 30.7, 28.5, 9.9. MS (ESI) *m/z* 484 $[M+H]^+$. HRMS (FAB) calc. for $C_{24}H_{33}N_7O_2S$ $[M+H]^+$ 484.2495, found 484.2502.

1-(4-(4-(6-Aminopyridin-2-yl)butoxy)-3-methoxyphenyl)-3-(3-(5-methyl-1*H*-imidazol-1-yl)propyl)thiourea (216). From compound **166**, procedure **7**. yield 55%, white solid, mp 95-96 ^{o}C. ^{1}H NMR (300 MHz, CD_3OD) δ 7.58 (d, J = 0.93 Hz, 1H), 7.38 (dd, J = 8.25, 7.32 Hz, 1H), 6.93 (d, J = 8.43 Hz, 1H), 6.88 (d, J = 2.37 Hz, 1H), 6.75 (dd, J = 8.40, 2.40 Hz, 1H), 6.65 (s, 1H), 6.50 (d, J = 7.32 Hz, 1H), 6.39 (d, J = 8.25 Hz, 1H), 4.02-3.94 (m, 4H), 3.80 (s, 3H), 3.61 (t, J = 7.14 Hz, 2H), 2.64 (t, J = 6.96 Hz, 2H), 2.21 (d, J = 0.93 Hz, 3H), 2.07 (quintet, J = 6.96 Hz, 2H), 1.82 - 1.79 (m, 4H). ^{13}C (100 MHz, CD_3OD) δ 183.3, 161.5, 161.3, 152.2, 149.4, 140.4, 138.8, 133.0, 129.7, 127.4, 119.8, 115.8, 113.6, 112.2, 108.3, 71.0, 57.3, 44.2, 43.8, 39.0, 32.2, 30.7, 28.3, 9.9. MS (ESI) *m/z* 469 $[M+H]^+$. HRMS (FAB) calc. for $C_{24}H_{32}N_6O_2S$ $[M + H]^+$ 469.2385, found 469.2378.

1-(3-Methoxy-4-(3-(pyrimidin-5-yl)propoxy)phenyl)-3-(3-(5-methyl-1*H*-imidazol-1-yl)propyl)thiourea (217). From compound **120**, procedure **5**. yield 66%, white solid, mp 298-299 ^{o}C. ^{1}H NMR (400 MHz, CD_3OD) δ 8.97 (s, 1H), 8.69 (s, 2H), 7.58 (d, J = 0.68 Hz, 1H), 6.93-6.91 (m, 2H), 6.76 (dd, J = 8.52, 2.40 Hz, 1H), 6.66 (br, 1H), 4.03 (t, J = 3.84 Hz, 2H), 3.99 (t, J = 7.28 Hz, 2H), 3.81 (s, 3H), 3.61 (t, J = 6.92 Hz, 2H), 2.91 (t, J = 7.36 Hz, 2H), 2.21 (d, J = 0.72 Hz, 3H), 2.17 (quintet, J = 6.08 Hz, 2H), 2.07 (quintet, J = 7.16 Hz, 2H). ^{13}C NMR (75 MHz, CD_3OD) δ 183.3, 158.9, 157.7, 152.0, 148.7, 138.6, 137.7, 133.3, 129.5, 127.3, 119.6, 115.8, 111.9, 69.8, 57.2, 44.1, 43.7, 32.1, 31.7, 28.5, 9.9. MS (FAB) *m/z* 441 $[M+H]^+$. HRMS (FAB) calc. for $C_{22}H_{28}N_6O_2S$ $[M + H]^+$ 441.2072, found 441.2067.

1-(3-Methoxy-4-(4-(pyrimidin-5-yl)butoxy)phenyl)-3-(3-(5-methyl-1*H*-imidazol-1-yl)propyl)thiourea (218). From compound **121**, procedure **5**. yield 48%, white solid, mp 104-

105 °C. ^{1}H NMR (300 MHz, CD_3OD) δ 8.97 (s, 1H), 8.70 (s, 2H), 7.59 (s, 1H), 6.94 (d, J = 8.58 Hz, 1H), 6.90 (d, J = 2.22 Hz, 1H), 6.75 (dd, J = 8.43, 2.37 Hz, 1H), 6.66 (br, 1H), 4.05 (t, J = 5.67 Hz, 2H), 3.99 (t, J = 7.32 Hz, 2H), 3.81 (s, 3H), 3.61 (t, J = 6.78 Hz, 2H), 2.79 (t, J = 6.93 Hz, 2H), 2.21 (d, J = 0.72 Hz, 3H), 2.07 (quintet, J = 7.14 Hz, 2H), 1.85-1.83 (m, 4H). ^{13}C NMR (75 MHz, CD_3OD) δ 183.3, 158.9, 157.7, 152.1, 149.2, 138.8, 138.4, 133.2, 129.7, 127.4, 119.8, 115.7, 112.1, 70.8, 57.3, 44.2, 43.9, 32.2, 31.5, 30.3, 29.3, 9.9. MS (FAB) *m/z* 455 $[M+H]^+$. HRMS (FAB) calc. for $C_{23}H_{30}N_6O_2S$ $[M + H]^+$ 455.2229, found 455.2229.

1-(4-(3-(2-Aminopyrimidin-5-yl)propoxy)-3-methoxyphenyl)-3-(3-(5-methyl-1*H*-imidazol-1-yl)propyl)thiourea (219). From compound **164**, procedure **7**. yield 45%, white solid, mp 88-89 °C. ^{1}H NMR (300 MHz, CD_3OD) δ 8.15 (s, 2H), 7.58 (s, 1H), 6.94-6.91 (m, 2H), 6.75 (d, J = 8.43, 2.37 Hz, 1H), 6.66 (br, 1H), 4.00-3.94 (m, 4H), 3.82 (s, 3H), 3.62 (t, J = 7.14 Hz, 2H), 2.69 (t, J = 7.14 Hz, 2H), 2.21 (d, J = 0.90 Hz, 3H), 2.05-2.01 (m, 4H). ^{13}C NMR (125 MHz, CD_3OD) δ 183.3, 164.0, 160.1, 152.2, 149.1, 138.8, 133.2, 129.7, 127.4, 125.5, 119.8, 115.9, 112.1, 69.8, 57.3, 44.2, 43.8, 32.3, 32.2, 27.5, 9.9. MS (FAB) *m/z* 456 $[M+H]^+$. HRMS (FAB) calc. for $C_{22}H_{29}N_7O_2S$ $[M + H]^+$ 456.2181, found 456.2187.

1-(4-(4-(2-Aminopyrimidin-5-yl)butoxy)-3-methoxyphenyl)-3-(3-(5-methyl-1*H*-imidazol-1-yl)propyl)thiourea (220). From compound **165**, procedure **7**. yield 77%, white solid, mp 74-75 °C. ^{1}H NMR (300 MHz, $CDCl_3$) δ 8.13 (s, 2H), 7.87 (s, 1H), 7.55 (s, 1H), 6.84 (d, J = 8.25 Hz, 1H), 6.75-6.71 (m, 3H), 6.24 (br, 1H), 4.98 (br, 2H), 4.04 (t, J = 6.03 Hz, 2H), 3.94 (t, J = 7.14 Hz, 2H), 3.82 (s, 3H), 3.67 (q, J = 6.60 Hz, 2H), 2.55 (t, J = 7.53 Hz, 2H), 2.18 (d, J = 0.93 Hz, 3H), 2.09-2.01 (m, 2H), 1.88-1.71 (m, 4H). ^{13}C NMR (75 MHz, CD_3OD) δ 183.2, 163.8, 159.9,

151.9, 149.0, 138.7, 133.0, 129.8, 127.0, 126.2, 119.6, 115.6, 112.0, 70.9, 57.3, 44.3, 43.7, 32.0, 31.2, 30.7, 29.7, 9.9. MS (FAB) 470 $[M+H]^+$. HRMS (FAB) calc. for $C_{23}H_{31}N_7O_2S$ $[M + H]^+$ 470.2338, found 470.2331.

Computational study.

Protein structure preparation. The X-ray crystal structure of the human glutaminyl cyclase (PDB ID: 3PBB)[M-1] was selected and prepared using the Protein Preparation Wizard in Maestro v.9.2 (Schrödinger, LLC, NY, USA). During the preparation process, the bond orders were assigned, zero-order bonds to Zn^{2+} were created, and hydrogen atoms were added. All the hydrogen atoms were energy-minimized with the optimized potential for liquid simulation (OPLS) 2005 force field until the average root mean square deviation for hydrogen atoms reached 0.30 Å.

Ligand preparation. The protonation states of the ligand molecules were predicted using the pKa prediction module in ACD/I-Lab web server (ACD/Labs, Toronto, Ontario, Canada). At pH 7.4, the major form of **B7** was protonated at the D-region and that of **C10** is predicted to have neutral and protonated forms with a ratio of 2:1. The three-dimensional structures of the ligand molecules were generated by LigPrep v.2.8 in Maestro. The resulting structures were energy-minimized in implicit solvent with the OPLS 2005 force field in Maestro.

Glide standard precision (SP) docking. The prepared ligand molecules were docked to hQC using Glide v.6.1 in Maestro. The grid for the active site was generated using the centroid of the co-crystallized ligand, PBD150, and the grid box size was set as the default value. The metal

coordination constraint was set as tetrahedral geometry for the Zn^{2+}. For the initial docking stage, Glide SP docking was performed with the maximum number of 30 poses per ligand.

Glide quantum mechanics polarized ligand docking (QPLD). The top 5 poses for each ligand from the previous Glide SP docking were selected and used for the following QPLD process. The partial charges of the docked ligands were calculated using Jaguar with the option of an accurate QM level. Then, the ligands with the updated charges were re-docked using Glide extra precision (XP).

Refinement of the protein-ligand complex structure. The protein-ligand complexes obtained from the QPLD were taken for further optimization by the Refine Protein-Ligand Complex module in Prime v.3.4 in Maestro (Schrödinger, LLC, NY, USA). Local optimization refinement within 5 Å of the docked ligand was performed. During this process, the side chain conformations of the selected protein residues were predicted and minimized and subsequently minimized along with the docked ligand. The results were further energy-minimized using a Monte Carlo sampling algorithm in 6000 steps. All the molecular graphic figures were generated by PyMOL software (http://www.pymol.org). All computational studies were undertaken on an Intel Xeon Octa-Core 2.5 GHz workstation with Linux CentOS release 5.8.

Biological Study.

In vitro QC activity assay. For testing the inhibition activities of test compounds, QC activity was fluorometrically evaluated. The used buffer consisted of 25 mM HEPES (Sigma), with pH 7.0, adjusted with HCl. The substrate H-Gln-AMC hydrobromide (L-glutamine 7-amido-4-

methylcoumarin, BACHEM, Switzerland) was use in a concentration of 0.4 mM. The auxiliary enzyme pGAPase (50 units, Qiagen, Germany) was prediluted 1:250 in HEPES. The human QC (10 μg/ml, rhQPCT, R&D systems) was prediluted 1:250 in HEPES. A typical reaction mixture consisted of 25 μL of substrate, 50 μL of the test compounds and 25 μL of pGAPase. After incubation in 96-well black plates (Greiner, Austria) for 10 min at 37 °C the reaction was started by adding 50 μL of the *h*QC solution.

Cytotoxicity assays. HT-22 (mouse hippocampal cells) cells were grown in Dulbecco's Modified Eagle's Medium (DMEM, GIBCO) supplemented with 10% (vol/vol) fetal bovine serum and antibiotics (100 mg/ml penicillin/streptomycin mix) in a humidified atmosphere at 37 ^{o}C with 5% CO_2. 5000 HT-22 cells per well were seeded into a clear 96-well plate one day prior to assay. Medium was removed from the plate, and cells were treated with 25μL solution of each compound at 10 μM and incubated at 37 ^{o}C for 18 h. 15 μL of 3-[4,5-dimethylthiazol-2-yl]-2,5-diphenyltetrazolium bromide (MTT) solution (5 mg/mL) was added to each well and incubated for 3 h. The formazan formed was dissolved in dimethyl sulfoxide (DMSO) and absorbance at 570 nm was measured using a microplate reader (Sunrise, TECAN). OD values from each well were subtracted with vehicle control and cell viability was calculated by using the signals from vehicle control as 100%.

Permeability assay. Parallel Artificial Membrane Permeability Assay (PAMPA)-BBB studies were conducted using the PAMPA Explorer kit (*p*ION Inc.). Stock solutions of all compounds were prepared in dimethyl sulfoxide (DMSO) (10 mM). Each stock solution was diluted to 50 μL (Final DMSO concentration 1%) in pH 7.4 Prisma HT buffer (*p*ION) and 200 μL were added to

each well of the donor plate (n=3). The polyvinylidene fluoride (PVDF, 0.45 μm) filter membrane on the acceptor plate was coated with 5 μL of BBB-1 lipid (*p*ION) formulation and to each well of the acceptor plate, 200 μL of brain sink buffer (BSB, *p*ION) was added. The acceptor filter plate was carefully placed on top of the donor plate to form a "sandwich". The sandwich was incubated at 25 °C for 4 h, without stirring. UV-vis spectra of the solutions in the reference, acceptor, and donor plates were measured using a microplate reader, Safire (Tecan, Switzerland). For each compound, -logP_e was calculated using the PAMPA Explorer software v.3.5 (*p*ION).

Animals and treatment. For acute model study, ICR mice were utilized. ICR mice were obtained from SAMTACO (Korea). Five microgram in five microliter of human $A\beta_{3-40}$ (62-0-99, American peptide) in PBS was injected into the deep cortical/hippocampus to 5 weeks old ICR mice (25 g, n = 4, male) using stereotaxic frame (myNeuroLab, USA). Test compounds were administrated via deep cortical/hippocampus or i.p. injection. After mice were anaesthetized with Zoletil50 and 2% Rumpun (1:2 ratio, 0.4 mL/kg) i.m., the animal was placed into a stereotaxic frame. A small incision (1 cm) was made over the midline of the skull and exposed the landmarks of the cranium (bregma and lambda). A small hole was drilled through the skull. Human $A\beta_{3-40}$ was injected into the deep cortical/hippocampus by using the following coordinates : AP -2.0 mm, ML 1.2 mm, DV 1.0 mm from the bregma. Using a Hamilton 25 μL syringe with 27-gauge guide needle, a 5 μL volume containing human Aβ3−40 was delivered.

For brain infusion study, APP/PS1 AD model Tg mice were obtained from Jackson lab (USA).

For continuous delivering of our compound, we performed implantation of miniosmotic pumps (ALZET) for in vivo delivery. Briefly, mice were anesthetized with and placed in a stereotactic

frame. A brain-infusion cannula (Brain Infusion Kit 3; ALZET, Cupertino, CA, USA) coupled via vinyl tubing to the osmotic pump was implanted into the deep cortical/ hippocampus (AP -2.0 mm, ML 1.2 mm, DV 1.0 mm from the bregma.). The test compounds were infused into the brain of APP/PS1 mice for 3 weeks.

For transgenic mice model study, a total of 12 (n=6 for vehicle; n=6 for compound treatment) 5XFAD mice (Jackson lab, ME) was utilized. 5XFAD mice co-express a total of five FAD mutations, including APP with three FAD mutations [K670N/M671L (Swedish), I716V (Florida) and V717I (London)] and PS1 with two mutations (M146L and L286V) under the control of neuronal specific Thy1 promoter. In this study, we followed the national guidelines in conducting animal experiments. All procedures for animal tests were approved by the Medifron Animal Care and Use Committee (approval number, Medifron 2013-2, IACUC). All surgical procedures were performed with care to minimize pain and discomfort. To evaluate the test compounds on AD model mice, the test compounds were administrated via intraperitoneal injection to mice to 19 week old male 5xFAD mice for 3 months. Mice were housed individually with a 12:12 h light: dark cycle (07:00–19:00 hours). The cognitive function of each mouse was measured after 3 months of administration.

Morris Water Maze (MWM) Test. The MWM was conducted during last 6 days of treatment period. The mouse had to find the hidden platform (10 cm in diameter) during 60 seconds trials in a circular pool with a diameter of 120 cm filled with opaque water at temperature of 22±1 °C. After each trial, mice were allowed to rest on the platform for 10 sec. All mice were given four training trials per day for 5 consecutive days. Escape latency, pathway and presence of the mice in the platform quadrant were quantified. 24 hours after the hidden-platform trial, mice were subjected to a probe trial in which the platform was removed, and their swimming paths were

recorded for 60 sec. All mice behavior (time/distance for reaching the platform, swimming speed, path length, and time spent in each quadrant) were quantified with EthoVision XT 7.0 software (Noldus information technology, Germany)

Aβ Sandwich ELISAs. Sandwich ELISA was performed for the quantification of N3pE-40 (for acute model mouse brain), $A\beta_{42}$ (for TG mouse brain), and N3pE-42 (for TG mouse brain). The mouse brains were completely lysed with RIPA buffer using a sonicator (SONICS, USA), and ultracentrifuged at 100,000 x g, 4°C for 1 h. The supernatant obtained here was RIPA-soluble fraction. The pellet was resuspended in 70% formic acid and ultracentrifuged under the same condition. The supernatant was collected as formic acid-soluble fraction. Protein concentrations were determined using a BCA kit (Thermo scientific). Sample duplicates were then run on $A\beta_{42}$ and N3pE-42 Aβ specific sandwich ELISAs following the protocol of the manufacturer (#27418 for N3pE-40, #27711 for $A\beta_{42}$, #27716 for N3pE-42, IBL Japan). Optical densities at 450 nm of each well were read on a plate reader, Safire (Tecan, Switzerland). The concentration of the sample $A\beta_{42}$ and N3pE-42 Aβ were determined by their standard curves. All readings were in the linear range of the assay. The concentration values were normalized to total brain weight and expressed in pg or ng of Aβ per mg of total protein. After the average of the duplicates was determined, the mean and SEM for each group were calculated.

Statistical Analyses. Data was expressed as mean ± SEM. All experiments were repeated at least 3 times. Statistical analyses between groups were performed using SPSS software(SPSS, Chicago, IL). For group comparisons of variables, we analyzed data with either One-way ANOVA with Bonferroni post-hoc test or independent samples t-test in SPSS. (ns: $p > 0.05$, * : $p < 0.05$, ** : $p < 0.01$,*** : $p < 0.001$)

■ ASSOCIATED CONTENT

Supporting Information

The figures of molecular modeling and the HPLC purities of all final compounds. This material is available free of charge via the Internet at http://pubs.acs.org.

■ AUTHOR INFORMATION

Corresponding Author

*Phone: 82-2-880-7846. Fax: 82-2-888-0649. E-mail: jeewoo@snu.ac.kr

Notes

The authors declare no competing financial interest.

■ ACKNOWLEDGEMENT

This work was supported by the Korea Science and Engineering Foundation (KOSEF) grants from the Korea government (MOST) (NRF-2014M3A9D9069725) and National Leading Research Lab (NLRL) program (2011-0028885).

■ ABBREVIATIONS USED

Aβ, β-amyloid; AD, Alzheimer's disease; AchEI, acetylcholineesterase inhibitors; APP, amyloid precursor protein; NMDA, *N*-methyl-D-aspartate; pGlu, pyroglutamate; QC, glutamyl cyclase

■ REFERENCES

(1) Hardy, J.; Selkoe, D. J. The amyloid hypothesis of Alzheimer's disease: progress and problems on the road to therapeutics. *Science* **2002,** *297*, 353-356.

(2) Bishop, G. M.; Robinson, S. R. Physiological roles of amyloid-beta and implications for its removal in Alzheimer's disease. *Drugs Aging* **2004,** *21*, 621-630.

(3) Puzzo, D.; Arancio, O. Amyloid-beta peptide: Dr. Jekyll or Mr. Hyde? *J. Alzheimer's Dis.* **2013,** *33 Suppl 1*, S111-120.

(4) Lopez-Toledano, M. A.; Shelanski, M. L. Neurogenic effect of beta-amyloid peptide in the development of neural stem cells. *J. Neurosci.* **2004,** *24*, 5439-5444.

(5) Yankner, B. A.; Duffy, L. K.; Kirschner, D. A. Neurotrophic and neurotoxic effects of amyloid beta protein: reversal by tachykinin neuropeptides. *Science* **1990,** *250*, 279-282.

(6) Giuffrida, M. L.; Caraci, F.; Pignataro, B.; Cataldo, S.; De Bona, P.; Bruno, V.; Molinaro, G.; Pappalardo, G.; Messina, A.; Palmigiano, A.; Garozzo, D.; Nicoletti, F.; Rizzarelli, E.; Copani, A. Beta-amyloid monomers are neuroprotective. *J. Neurosci.* **2009,** *29*, 10582-10587.

(7) Giuffrida, M. L.; Caraci, F.; De Bona, P.; Pappalardo, G.; Nicoletti, F.; Rizzarelli, E.; Copani, A. The monomer state of beta-amyloid: where the Alzheimer's disease protein meets physiology. *Rev. Neurosci.* **2010,** *21*, 83-93.

(8) Butterfield, D. A. Amyloid beta-peptide (1-42)-induced oxidative stress and neurotoxicity: implications for neurodegeneration in Alzheimer's disease brain. A review. *Free Radical Res.* **2002,** *36*, 1307-1313.

(9) Baruch-Suchodolsky, R.; Fischer, B. Abeta40, either soluble or aggregated, is a remarkably potent antioxidant in cell-free oxidative systems. *Biochemistry* **2009,** *48*, 4354-4370.

(10) Soscia, S. J.; Kirby, J. E.; Washicosky, K. J.; Tucker, S. M.; Ingelsson, M.; Hyman, B.; Burton, M. A.; Goldstein, L. E.; Duong, S.; Tanzi, R. E.; Moir, R. D. The Alzheimer's disease-associated amyloid beta-protein is an antimicrobial peptide. *PLoS One* **2010,** *5*, e9505.

(11) Larner, A. J. Hypothesis: amyloid beta-peptides truncated at the N-terminus contribute to the pathogenesis of Alzheimer's disease. *Neurobiol. Aging* **1999,** *20*, 65-69.

(12) Kumar-Singh, S.; De Jonghe, C.; Cruts, M.; Kleinert, R.; Wang, R.; Mercken, M.; De Strooper, B.; Vanderstichele, H.; Lofgren, A.; Vanderhoeven, I.; Backhovens, H.; Vanmechelen, E.; Kroisel, P. M.; Van Broeckhoven, C. Nonfibrillar diffuse amyloid deposition due to a gamma(42)-secretase site mutation points to an essential role for N-truncated A beta(42) in Alzheimer's disease. *Hum. Mol. Genet.* **2000,** *9*, 2589-2598.

(13) Miravalle, L.; Calero, M.; Takao, M.; Roher, A. E.; Ghetti, B.; Vidal, R. Amino-terminally truncated Abeta peptide species are the main component of cotton wool plaques. *Biochemistry* **2005,** *44*, 10810-10821.

(14) Jawhar, S.; Wirths, O.; Bayer, T. A. Pyroglutamate amyloid-beta (Abeta): a hatchet man in Alzheimer disease. *J. Biol. Chem.* **2011,** *286*, 38825-38832.

(15) Saido, T. C.; Iwatsubo, T.; Mann, D. M.; Shimada, H.; Ihara, Y.; Kawashima, S. Dominant and differential deposition of distinct beta-amyloid peptide species, A beta N3(pE), in senile plaques. *Neuron* **1995,** *14*, 457-466.

(16) Schlenzig, D.; Manhart, S.; Cinar, Y.; Kleinschmidt, M.; Hause, G.; Willbold, D.; Funke, S. A.; Schilling, S.; Demuth, H. U. Pyroglutamate formation influences solubility and amyloidogenicity of amyloid peptides. *Biochemistry* **2009,** *48*, 7072-7078.

(17) Russo, C.; Violani, E.; Salis, S.; Venezia, V.; Dolcini, V.; Damonte, G.; Benatti, U.; D'Arrigo, C.; Patrone, E.; Carlo, P.; Schettini, G. Pyroglutamate-modified amyloid beta-peptides-

-AbetaN3(pE)--strongly affect cultured neuron and astrocyte survival. *J. Neurochem.* **2002,** *82*, 1480-1489.

(18) He, W.; Barrow, C. J. The A beta 3-pyroglutamyl and 11-pyroglutamyl peptides found in senile plaque have greater beta-sheet forming and aggregation propensities in vitro than full-length A beta. *Biochemistry* **1999,** *38*, 10871-10877.

(19) Nussbaum, J. M.; Schilling, S.; Cynis, H.; Silva, A.; Swanson, E.; Wangsanut, T.; Tayler, K.; Wiltgen, B.; Hatami, A.; Ronicke, R.; Reymann, K.; Hutter-Paier, B.; Alexandru, A.; Jagla, W.; Graubner, S.; Glabe, C. G.; Demuth, H. U.; Bloom, G. S. Prion-like behaviour and tau-dependent cytotoxicity of pyroglutamylated amyloid-beta. *Nature* **2012,** *485*, 651-655.

(20) Busby, W. H., Jr.; Quackenbush, G. E.; Humm, J.; Youngblood, W. W.; Kizer, J. S. An enzyme(s) that converts glutaminyl-peptides into pyroglutamyl-peptides. Presence in pituitary, brain, adrenal medulla, and lymphocytes. *J. Biol. Chem.* **1987,** *262*, 8532-8536.

(21) Bockers, T. M.; Kreutz, M. R.; Pohl, T. Glutaminyl-cyclase expression in the bovine/porcine hypothalamus and pituitary. *J. Neuroendocrinol.* **1995,** *7*, 445-453.

(22) Pohl, T.; Zimmer, M.; Mugele, K.; Spiess, J. Primary structure and functional expression of a glutaminyl cyclase. *Proc. Natl. Acad. Sci. U. S. A.* **1991,** *88*, 10059-10063.

(23) Morawski, M.; Schilling, S.; Kreuzberger, M.; Waniek, A.; Jager, C.; Koch, B.; Cynis, H.; Kehlen, A.; Arendt, T.; Hartlage-Rubsamen, M.; Demuth, H. U.; Rossner, S. Glutaminyl cyclase in human cortex: correlation with (pGlu)-amyloid-beta load and cognitive decline in Alzheimer's disease. *J. Alzheimer's Dis.* **2014,** *39*, 385-400.

(24) Schilling, S.; Zeitschel, U.; Hoffmann, T.; Heiser, U.; Francke, M.; Kehlen, A.; Holzer, M.; Hutter-Paier, B.; Prokesch, M.; Windisch, M.; Jagla, W.; Schlenzig, D.; Lindner, C.; Rudolph, T.; Reuter, G.; Cynis, H.; Montag, D.; Demuth, H. U.; Rossner, S. Glutaminyl cyclase inhibition

attenuates pyroglutamate Abeta and Alzheimer's disease-like pathology. *Nat. Med.* **2008,** *14*, 1106-1111.

(25) Jawhar, S.; Wirths, O.; Schilling, S.; Graubner, S.; Demuth, H. U.; Bayer, T. A. Overexpression of glutaminyl cyclase, the enzyme responsible for pyroglutamate A{beta} formation, induces behavioral deficits, and glutaminyl cyclase knock-out rescues the behavioral phenotype in 5XFAD mice. *J. Biol. Chem.* **2011,** *286*, 4454-4460.

(26) Schilling, S.; Appl, T.; Hoffmann, T.; Cynis, H.; Schulz, K.; Jagla, W.; Friedrich, D.; Wermann, M.; Buchholz, M.; Heiser, U.; von Horsten, S.; Demuth, H. U. Inhibition of glutaminyl cyclase prevents pGlu-Abeta formation after intracortical/hippocampal microinjection in vivo/in situ. *J. Neurochem.* **2008,** *106*, 1225-1236.

(27) Lues, I.; Weber, F.; Meyer, A.; Bühring, U.; Hoffmann, T.; Kühn-Wache, K.; Manhart, S.; Heiser, U.; Pokorny, R.; Chiesa, J. A phase 1 study to evaluate the safety and pharmacokinetics of PQ912, a glutaminyl cyclase inhibitor, in healthy subjects. *Alzheimer's Dement.* **2015,** *1*, 182-195.

(28) Buchholz, M.; Hamann, A.; Aust, S.; Brandt, W.; Bohme, L.; Hoffmann, T.; Schilling, S.; Demuth, H. U.; Heiser, U. Inhibitors for human glutaminyl cyclase by structure based design and bioisosteric replacement. *J. Med. Chem.* **2009,** *52*, 7069-7080.

(29) Buchholz, M.; Heiser, U.; Schilling, S.; Niestroj, A. J.; Zunkel, K.; Demuth, H. U. The first potent inhibitors for human glutaminyl cyclase: synthesis and structure-activity relationship. *J. Med. Chem.* **2006,** *49*, 664-677.

(30) Li, M.; Dong, Y.; Yu, X.; Zou, Y.; Zheng, Y.; Bu, X.; Quan, J.; He, Z.; Wu, H. Inhibitory effect of flavonoids on human glutaminyl cyclase. *Bioorg. Med. Chem.* **2016,** *24*, 2280-2286.

(31) Ramsbeck, D.; Buchholz, M.; Koch, B.; Bohme, L.; Hoffmann, T.; Demuth, H. U.; Heiser, U. Structure-activity relationships of benzimidazole-based glutaminyl cyclase inhibitors featuring a heteroaryl scaffold. *J. Med. Chem.* **2013,** *56*, 6613-6625.

(32) Tran, P. T.; Hoang, V. H.; Thorat, S. A.; Kim, S. E.; Ann, J.; Chang, Y. J.; Nam, D. W.; Song, H.; Mook-Jung, I.; Lee, J.; Lee, J. Structure-activity relationship of human glutaminyl cyclase inhibitors having an N-(5-methyl-1H-imidazol-1-yl)propyl thiourea template. *Bioorg. Med. Chem.* **2013,** *21*, 3821-3830.

(33) Efange, S. M.; Michelson, R. H.; Knusel, B.; Hefti, F.; Boudreau, R. J.; Thomas, J. R.; Tennison, J. R. Synthesis and biological evaluation of radioiodinated N-2-(4-piperidyl)ethyl benzamides. *Nucl. Med. Biol.* **1993,** *20*, 527-538.

(34) Bautista-Aguilera, O. M.; Samadi, A.; Chioua, M.; Nikolic, K.; Filipic, S.; Agbaba, D.; Soriano, E.; de Andres, L.; Rodriguez-Franco, M. I.; Alcaro, S.; Ramsay, R. R.; Ortuso, F.; Yanez, M.; Marco-Contelles, J. N-Methyl-N-((1-methyl-5-(3-(1-(2-methylbenzyl)piperidin-4-yl)propoxy)-1H-indol-2- yl)methyl)prop-2-yn-1-amine, a new cholinesterase and monoamine oxidase dual inhibitor. *J. Med. Chem.* **2014,** *57*, 10455-10463.

(35) Kurosawa, W.; Kan, T.; Fukuyama, T. Preparation of secondary amines from primary amines via 2-nitrobenzenesulfonamides: N-(4-methoxybenzyl)-3-phenylpropylamine. *Org. Synth.* **2003**, 186-186.

(36) Nettekoven, M. Combinatorial synthesis of 5-aryl-[1, 2, 4]-triazolo-[1, 5-a]-pyridine derivatives as potential inhibitors of the adenosine 2a receptor. *Synlett* **2001,** *2001*, 1917-1920.

(37) Schilling, S.; Hoffmann, T.; Wermann, M.; Heiser, U.; Wasternack, C.; Demuth, H. U. Continuous spectrometric assays for glutaminyl cyclase activity. *Anal. Biochem.* **2002,** *303*, 49-56.

(38) Koch, B.; Buchholz, M.; Wermann, M.; Heiser, U.; Schilling, S.; Demuth, H. U. Probing secondary glutaminyl cyclase (QC) inhibitor interactions applying an in silico-modeling/site-directed mutagenesis approach: implications for drug development. *Chem. Biol. Drug Des.* **2012,** *80*, 937-946.

(39) Becker, A.; Eichentopf, R.; Sedlmeier, R.; Waniek, A.; Cynis, H.; Koch, B.; Stephan, A.; Bauscher, C.; Kohlmann, S.; Hoffmann, T.; Kehlen, A.; Berg, S.; Freyse, E. J.; Osmand, A.; Plank, A. C.; Rossner, S.; von Horsten, S.; Graubner, S.; Demuth, H. U.; Schilling, S. IsoQC (QPCTL) knock-out mice suggest differential substrate conversion by glutaminyl cyclase isoenzymes. *Biol. Chem.* **2016,** *397*, 45-55.

(40) Oakley, H.; Cole, S. L.; Logan, S.; Maus, E.; Shao, P.; Craft, J.; Guillozet-Bongaarts, A.; Ohno, M.; Disterhoft, J.; Van Eldik, L.; Berry, R.; Vassar, R. Intraneuronal beta-amyloid aggregates, neurodegeneration, and neuron loss in transgenic mice with five familial Alzheimer's disease mutations: potential factors in amyloid plaque formation. *J. Neurosci.* **2006,** *26*, 10129-10140.

(41) Hwang, J. Y.; Huang, W.; Arnold, L. A.; Huang, R.; Attia, R. R.; Connelly, M.; Wichterman J.; Zhu, F.; Augustinaite, I.; Austin, C. P.; Inglese, J.; Johnson, R. L.; Guy, R. K. Methylsulfonylnitrobenzoates, a new class of irreversible inhibitors of the interaction of the thyroid hormone receptor and its obligate coactivators that functionally antagonizes thyroid hormone. *J. Biol. Chem.* **2011**, *286*, 11895–11908.

(42) Huang, K. F.; Liaw, S. S.; Huang, W. L.; Chia, C. Y.; Lo, Y. C.; Chen, Y. L.; Wang, A. H. Structures of human Golgi-resident glutaminyl cyclase and its complexes with inhibitors reveal a large loop movement upon inhibitor binding. *J. Biol. Chem.* **2011**, *286*, 12439-12449.

(43) Cho, A. E.; Guallar, V.; Berne, B. J.; Friesner, R. Importance of accurate charges in molecular docking: quantum mechanical/molecular mechanical (QM/MM) approach. *J. Comput. Chem.* **2005**, *26*, 915-931.

(44) Li, Z.; Scheraga, H. A. Monte Carlo-minimization approach to the multiple-minima problem in protein folding. *Proc. Natl. Acad. Sci. U. S. A.* **1987**, *84*, 6611-6615.

Table of Contents graphic

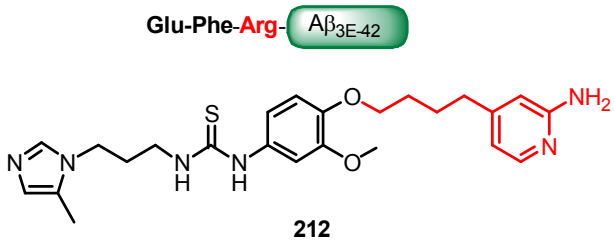

212

- EFR mimetic of $A\beta_{42}$
- hQC IC_{50} = 4.5 nM, mQC IC_{50} = 21.5 nM
- hIsoQC IC_{50} = 502 nM
- in vivo (ip) : 54.7% inh. of *h*$A\beta_{N3pE-42}$